# CHARACTERIZATION OF THE NON-STRUCTURAL PROTEINS OF ADENO-ASSOCIATED VIRUS (AAV) AND MINUTE VIRUS OF CANINE (MVC)

---

A Dissertation Presented to the Faculty of the Graduate School of the University of Missouri in Partial Fulfillment of Requirement for the Degree of Doctor of Philosophy

---

By

NOWATTEE LORETTA SUKHU

Dr. David Pintel, Mentor and Dissertation Advisor

December, 2012

The undersigned, appointed by the dean of the Graduate School, have examined the dissertation entitled

Characterization of the non-structural proteins of adeno-associated virus (AAV) and minute virus of canine (MVC)

Presented by N. Loretta Sukhu, a candidate for the degree of Doctor of Philosophy, and hereby certify that, in their opinion, it is worthy of acceptance.

Dr. David Pintel

Dr. Donsheng Duan

Dr. Marc Johnson

Dr. Bumsuk Hahm

Dr. Karen Bennett

# ACKNOWLEDGEMENTS

Foremost, I want to express my deepest gratitude to my advisor Dr. David Pintel for his guidance, support, patience, and kindness during the course of my Ph.D. work. Dr. Pintel's enthusiasm for science at its highest level is both contagious and inspirational especially during the difficult times. I have learned so very much. I also gratefully acknowledge the other members of my committee, Drs. Bennett, Duan, Johnson and Hahm, for their time and consideration.

I thank my labmates for their support and friendship over the years. Richard Adeyemi has been a good friend from the beginning and Olufemi Fasina who worked with me on the MVC project was generous and supportive. I especially thank Lisa Burger for the tremendous help she has given me.

I want to thank the professors who generously shared key reagents without which I would not have been able to do many of the experiments; Dr. Jianming Qiu who provided the MVC infectious clone, Dr. Colin Parrish for the MVC antibodies and virus, and Dr. Jude Samulski for the AAV Rep 78/68 hybridoma.

I am forever grateful to my family, Dan and Luke, for their endless support, encouragement, love, and patience especially when it was most needed. I could not have done it without you. I thank my parents for keeping me in their hearts and prayers every day.

# TABLE OF CONTENTS

Page Number

# LIST OF ABBREVIATIONS

| | |
|---|---|
| AAV | Adeno-associated virus |
| Ad | Adenovirus |
| AMDV | Aleutian Mink Disease Virus |
| ATP | Adenosine Triphosphate |
| Cul5 | Cullin 5 |
| DSE | Downstream element |
| EGFR-PTK | Epidermal growth factor protein tyrosine kinase |
| FKBP52 | a 52 kDa FK506 binding protein |
| GPV | Goose Parvovirus |
| HPV | Human Papilloma Virus |
| HSV | Herpes Simplex Virus |
| ITRs | Inverted terminal repeats |
| Kb | Kilobase |
| kDa | Kilodalton |
| MRN | MRE11-Rad50-Nbs1 |
| MVC | Minute Virus of Canine |
| NP1 | Nucleoprotein1 |
| NS | Non-strucutral |
| ORFs | Open reading frames |
| Rbx1 | Ring-box-1 |
| RNP | Ribonucleotide binding protein |
| RPA | Ribonuclease protection assay |
| ss DBP | Single-strand DNA binding protein |
| TC-TCP | T-cell protein tyrosine phosphatase |

| | |
|---|---|
| Ub | Ubiquitin |
| UPP | Ubiquitin Proteasome Pathway |
| USE | Upstream element |

# LIST OF FIGURES

## ABSTRACT

Parvoviruses are among the smallest of the animal DNA viruses. At the ends of the genome are inverted terminal repeats. The 5 kilobase genome encodes only two genes *rep* and *cap* that generate the viral proteins required for replication and virion assembly. As a consequence of this compact genome, parvovirus *rep* and *cap* display immense heterogeneity both in the mechanisms involved in gene expression and the functions of the encoded proteins.

The *rep* gene of adeno-associated virus type 2 (AAV2) encodes four non-structural proteins: Rep78, Rep68, Rep52, and Rep40. AAV2 large Rep proteins (Rep 78/68) provide a myriad of functions that are essential for AAV replication, including site specific endonuclease and helicase activities that are critical for AAV integration, DNA replication and specific activation of AAV promoters during transcription. It has also been shown that large Rep can inhibit expression of certain cellular and viral promoters, suppress adenovirus replication during co-infection and can have profound effects on cellular metabolism. Surprisingly, our knowledge of how the AAV large Rep protein is modified post-translationally is incomplete.

Five adenovirus (Ad) gene products are required for efficient replication of co-infecting adeno-associated virus (AAV); however, enhancement of AAV replication by these factors is composed of both positive and negative effects. Research presented in Chapter 2 revealed that AAV2 large Rep protein is targeted for ubiquitination and degradation by an E3 ubiquitin ligase complex which contains the Ad E4orf6, E1b 55k and cellular cullin 5 proteins. Additionally,

large Rep is also targeted for ubiquitination via extension of ubiquitin lysine K48 and K63 in both the absence and presence of E4orf6 and E1b 55k.

The bocavirus minute virus of canine (MVC) provides an excellent model to study infection and pathogenesis of members of the bocavirus genus. Data obtained from experiments with MVC may also be relevant to the closely related, potentially pathogenic, recently identified human bocavirus (HBoV). Previous work on MVC reported on the expression of two non-structural (NS) proteins, NS1 and NP1. Sequence analysis shows that expression of NP1 is unique among the bocavirus genus as this protein bears little homology with other parvoviral proteins. Work presented in Chapter 3 summarizes a comprehensive characterization of a single cycle infection with MVC in permissive canine WRD cells. This work identified a previously unreported smaller NS protein that is derived from a novel spliced mRNA within the larger NS gene.

In addition, in this work we also identified a role for the viral NP1 protein during infection. NP1 is required for read-through of the MVC internal polyadenylation site and thus, access to the capsid transcripts VP1 and VP2. Although the mechanism of NP1's action has not yet been fully elucidated, it represents the first parvovirus protein directly implicated in viral RNA processing.

# CHAPTER I

# LITERATURE REVIEW

## BIOLOGY OF *PARVOVIRIDAE*

Members of the *Parvoviridae* family are among the simplest and smallest DNA containing animal viruses. They all have a set of common features, which consist of non-enveloped virions with a diameter of 20 to 26 nm; linear, non-segmented, single-stranded genomes of approximately 5 kilobases in size which are encapsidated within icosahedral capsids. The termini of the genomes consist of palindromic sequences of approximately 115 nucelotides which are capable of forming hairpins. The terminal hairpin structures are important because they serve as origins of replication that are essential for genome replication (1).

The *Parvoviridae* family is further divided into two sub-families, *Parvovirinae* and the *Densovirinae* which infect vertebrate and invertebrate hosts, respectively. The *Densovirinae* subfamily encompasses four genera: densovirus, iteravirus, brevidensovirus, and pfudensovirus.

A phylogenetic map of the *Parvovirinae* is illustrated in Fig. 1-1. Among the *Parvovirinae* sub-family, commonly called the parvoviruses, there are two distinct types of viruses, replication-defective viruses which depend on a helper virus in order to achieve productive replication, and autonomous, replication competent viruses. The parvovirus, erythrovirus, amdovirus, and bocavirus genera comprise the autonomous *Parvovirinae* while the replication defective viruses are all members of the dependovirus genus (2).

**Figure 1-1 A phylogenetic map showing the autonomous and replication-defective genera of the family *Parvovirinae*.** There are 5 genera within the sub-family *Parvovirinae*. Parvovirus, Erythrovirus, Amdovirus and Bocavirus comprise the autonomously replicating genera while members of the Dependovirus genus require help from another larger DNA virus to achieve productive infection. Adapted from J.R. Kerr, S.F. Cotmore, M.E. Bloom, R.M. Linden, and C.R. Parrish (ed.), Parvoviruses, Hodder Arnold (2006), London, United Kingdom.

**Figure 1-1 A phylogenetic map showing the autonomous and replication-defective genera of the family *Parvovirinae*.**

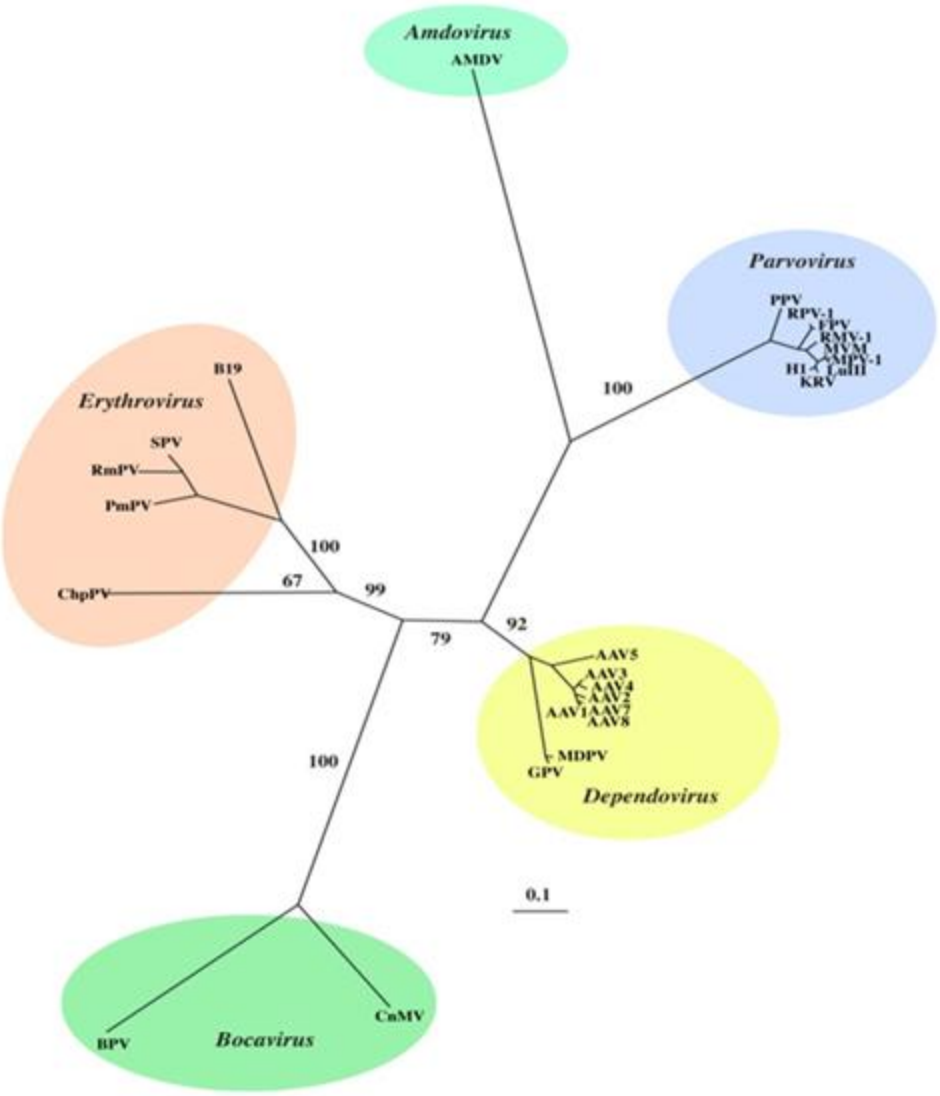

Parvovirus infections range from those that cause serious diseases such as parvovirus B19 to those which cause non-apparent subclinical infections such as adeno-associated virus (AAV). Novel research presented in this dissertation focuses on three members of the *Parvovirinae* sub-family, the minute virus of canine (MVC), a member of the bocavirus genus, and the type 2 and type 5 adeno-associated viruses (AAV), members of the dependovirus genus.

## GENERAL INTRODUCTION TO AAV

The first human adeno-associated virus (AAV) was discovered in 1965 as a contaminant of adenovirus (Ad) preparations (3). AAVs are among the smallest and simplest of the animal DNA viruses with a non-enveloped capsid of approximately 22 nm. Although 80-90% of adults are seropositive for AAV2, as noted above, infection with this virus has not been associated with any symptoms or disease. AAV is an attractive vector for gene therapy applications due to its lack of toxicity in vivo, availability of different serotypes, its ability to transduce a wide assortment of tissues and cell types and the ability to achieve long term expression without genome integration.

In order to achieve productive replication most members of the dependovirus genus, as their name implies, depend on the helper functions of a larger autonomously replicating DNA virus. Under certain conditions, such as treatment of host cells with DNA damaging agents, low-level replication can occur among some dependoviruses in the absence of helper virus (4). In addition, due to sequence similarities and the organization of their genomes the

autonomously replicating goose parvovirus and duck parvovirus are also members of the dependovirus genus.

A schematic of the life cycle of AAV, the prototypical member of the dependovirus genus is shown in Fig. 1-2. A larger more complex DNA virus, typically an adenovirus or a herpes virus, provides the helper components necessary for AAV replication. In the absence of a co-infecting virus, AAV2 (the prototypical AAV) site specifically integrates into the long arm of human chromosome 19 (5). Following integration, AAV2 can remain in a latent form until re-activation by either infection of the cell with a helper virus or DNA damage. Once either of these events occurs the virus can undergo a shift from latency to a lytic life cycle (Fig. 1-2). In the presence of a helper virus the genome can now productively replicate, resulting in the production of progeny virus (Fig. 1-2).

**Figure 1-2 The adeno-associated virus (AAV) life cycle.** Upon entry into the cell, in the absence of a helper virus, AAV can enter a latent life cycle where it integrates into the host chromosome. Upon super-infection with a helper virus, adenovirus, AAV can enter a lytic life cycle in which its genome is replicated,leading to the production of progeny virus. Taken from Kotin R (1994) Hum Gene Ther.

**Figure 1-2 The adeno-associated virus (AAV) life cycle.**

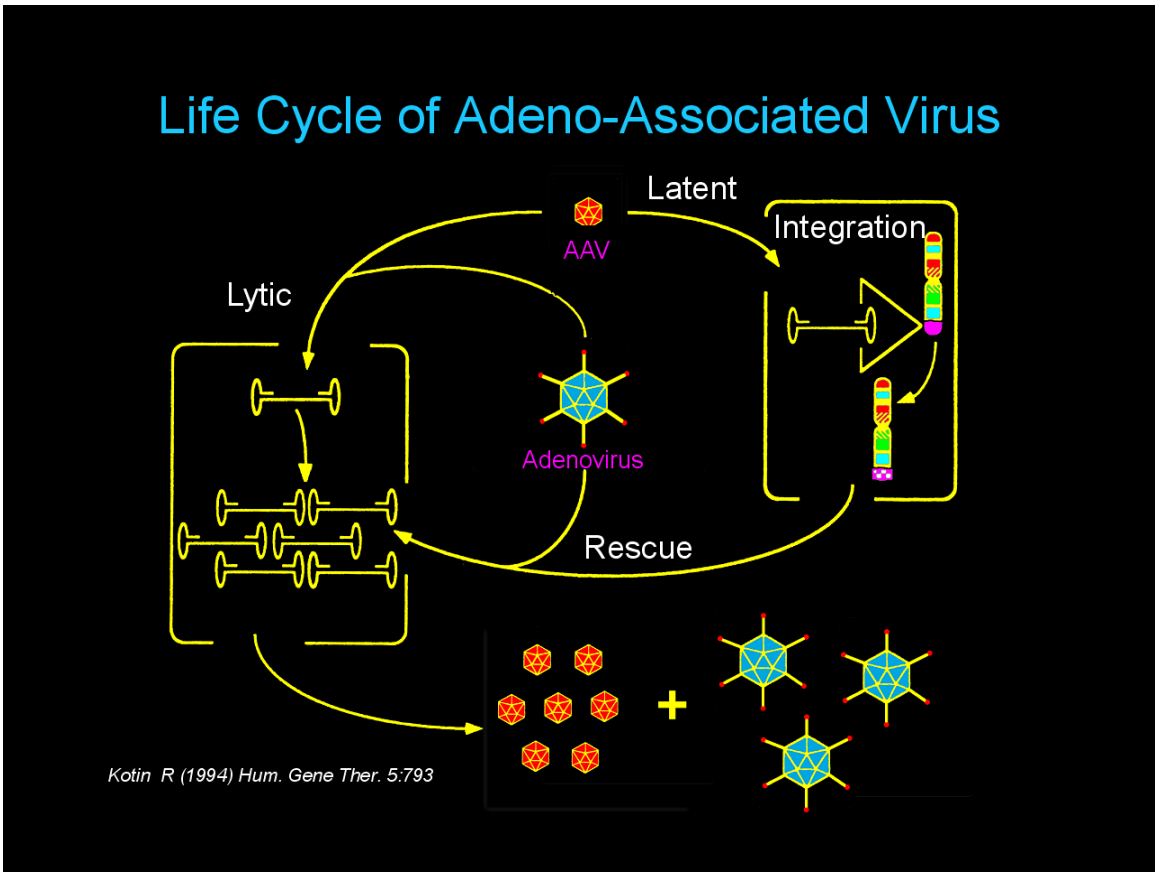

## TRANSCRIPTION PROFILE OF AAV2

The 4.7 kilobase (kb) genome of AAV consists of two viral genes, *rep* and *cap*, which encode replication and structural proteins, respectively. The open reading frames (ORFs) are flanked on each end by a 145 nucleotide long inverted terminal repeats (ITRs). Due to its compact genome, AAV2 like other parvoviruses, utilizes RNA processing strategies to maximize and regulate its gene expression (6). A schematic of the transcriptional profile of AAV2 is depicted in Fig. 1-3. The two open reading frames are organized into three transcriptional units with promoters at map units 5, (P5), 19 (P19), and 40 (P40). The use of multiple promoters and alternative splicing signals generates 6 major RNA species. Transcription initiation at P5 generates RNAs that encode the large non-structural proteins Rep78 and Rep68, while initiation at P19 produces RNAs that encode the small non-structural proteins Rep 52 and Rep40. The large and small rep proteins are alternatively spliced via an intron that resides in the middle of the genome. Splicing via this intron utilizes a single donor (D) and one of two acceptor sites (A1 or A2) as shown in Fig. 1-4. This results in the generation of either Rep 78 or Rep 52 from unspliced RNAs or Rep 68 and Rep 40 from spliced RNAs.

The P40 transcript encodes the capsid proteins, VP1 and VP2, which are alternatively spliced using the A1 or A2 acceptor sites, respectively. VP3 is a product of the spliced D/A2 transcript that utilizes a downstream translation initiation codon. Additionally, the capsid gene also encodes a small protein, the assembly accessory protein (AAP) that is involved in capsid assembly (7).

**Figure 1-3 Map of the AAV viral genome.** The 4.7 kb genome of AAV is flanked by two inverted terminal repeats (ITRs). The genome contains two open reading frames (ORFs) and three promoters. Using the three promoters and alternative splicing signals the virus can generate RNA species that encode rep and cap proteins. The rep ORF encodes four regulatory proteins (Rep 78, 68, 52, and 40) that are involved in AAV DNA replication, gene expression and packaging The cap ORF encodes four proteins, three that constitute the viral capsid (VP1, VP2 and VP3) and one additional small protein (AAP) that is involved in virion assembly. Figure taken from http://hvd.ens-lyon.fr/teams/AAV.

**Figure 1-3 Map of the AAV viral genome.**

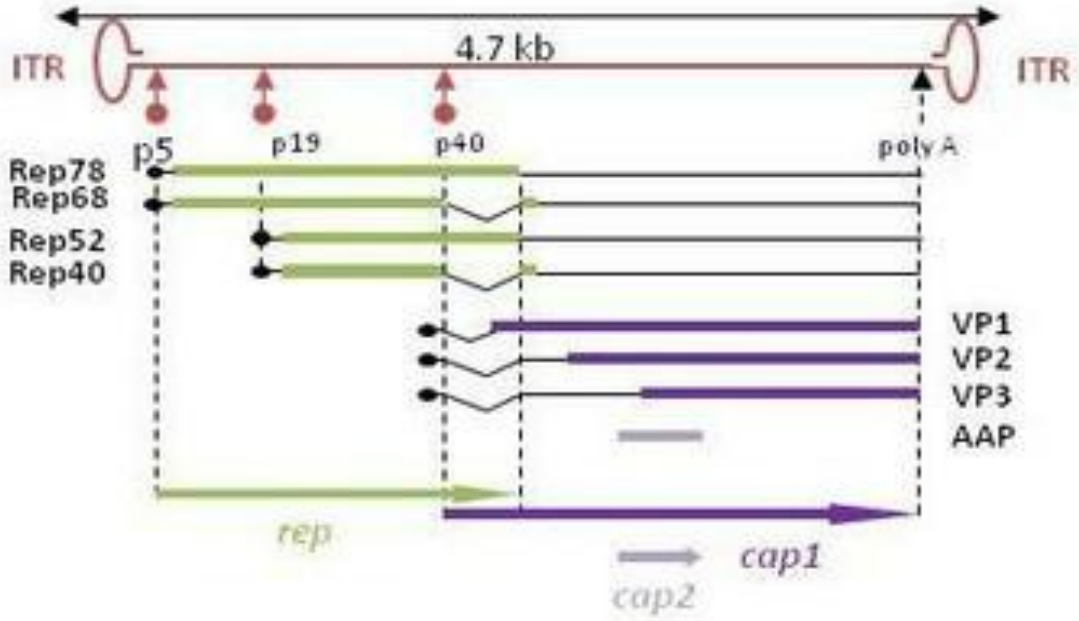

## TRANSCRIPTION PROFILE OF AAV5 RELATIVE TO AAV2

Although the genomes of AAV2 and AAV5 share many similarities, previous work done in the Pintel laboratory has demonstrated that there are several notable differences between AAV5 and AAV2 (6). The transcriptional map of AAV5 is shown in Fig. 1-4. AAV5, like AAV2, utilizes three promoters located at map units 7 (P7), 19 (P19) and 41 (P41). The P7 and P19 transcripts in AAV5 encode large and small non-structural proteins, respectively; the capsids proteins are generated from the P41 transcript. Unlike AAV2, AAV5 transcripts resulting from the P7 and P19 promoters undergo an early polyadenylation event using a proximal polyadenylation signal within the intron (pA)p thereby producing only Rep78 (from P7) and Rep52 (from P19). Inhibition of polyadenylation at the pA(p) is necessary for the read-through of P41 generated transcripts which are subsequently spliced to generate capsid mRNAs (6). The complex regulation of internal polyadenylation at (pA)p and splicing in AAV5 has been delineated and shown to be governed by the distance between the promoter and the intron. In addition, internal polyadenylation and splicing are inhibited by the host-derived U1 small nuclear ribonucleoprotein binding protein (RNP) binding to the intervening splice donor site (6). An increase in polyadenylation at the (pA)p site is observed as the distance is increased between the RNA initiation site, the intron, and the (pA)p site (6). Engineered mutations in the viral genome designed to interfere with splicing have been shown to result in an increase in polyadenylation at the (pA)p site indicating that splicing and polyadenylation events compete for the available pools of AAV5 mRNA (6).

**Figure 1-4 Transcription map of AAV5.** The AAV5 genome is shown at the bottom of the figure, and includes the location of the viral promoters (P7, P19, P41), the small intron donor (D) and acceptors (A1 and A2), the termination site for the Rep proteins, the internal polyadenlylation site (pA)p, and the inverted terminal repeats (ITRs). The major transcripts, and the proteins that they encode are shown above. The different open reading frames (ORFs) that are used are shown in different shading patterns. A transcription initiation site within the ITR is shown (Inr). It is not clear whether a portion of Inr-initiated RNA is spliced or not; this is indicated by a dashed line. Taken from Qiu *et al* Ch. 18 Parvovirus RNA Processing Strategies from J.R. Kerr, S.F. Cotmore, M.E. Bloom, R.M. Linden, and C.R. Parrish (ed.), Parvoviruses, Hodder Arnold (2006), London, United Kingdom.

**Figure 1-4 Transcription map of AAV5.**

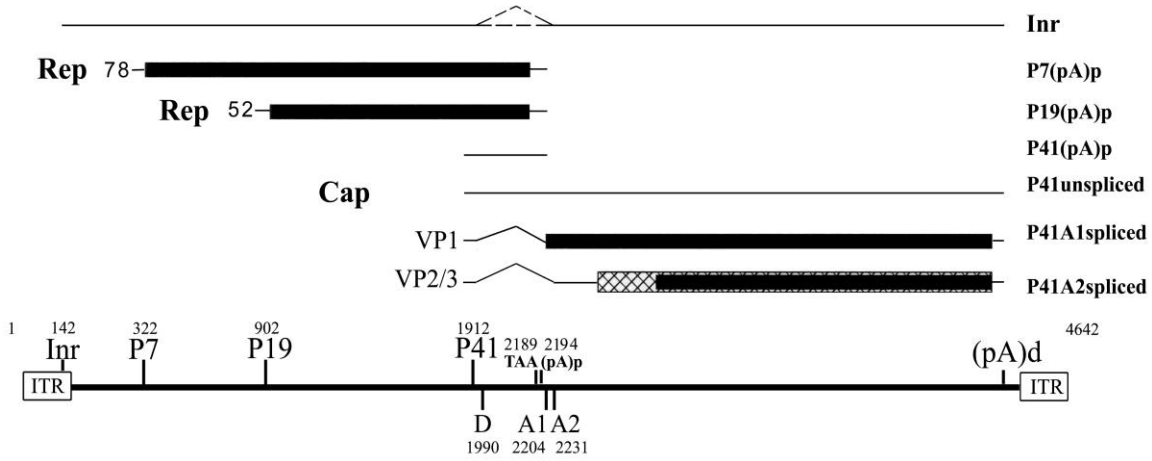

The Rep 40 protein in AAV2 is produced by alternative splicing of the P19 transcript. However, no such splicing events have been observed in the P19 transcript of AAV5. Recent work done in the Pintel laboratory has shown that AAV5 utilizes a novel alternative translation initiation codon to encode a small Rep 40 protein that is similar to the Rep 40 protein of AAV2 (8). In contrast to the differences noted in the production of the Rep proteins between AAV2 and AAV5 the capsid proteins of AAV5 are produced from the P41 transcript in a manner similar to that of AAV2.

## ADENOVIRUS HELPER GENE PRODUCTS REQUIRED FOR PRODUCTIVE AAV INFECTION

Productive AAV infection requires helper functions that can be supplied by co-infection with a larger DNA virus. Helper viruses can include members of the adenovirus, herpes simplex virus, vaccinia virus or human papillomavirus (HPV) families. One of the key roles these helper viruses provide in aiding AAV replication is by inducing modifications to, or alterations in, the localization of cellular proteins that are required to facilitate AAV replication (4).

Adenovirus type 5 (Ad5) provides five components that are essential for AAV replication; namely, E1a, E1b 55k, E2a, and E4orf6 proteins and the virus-associated (VA) RNA. Although the full extent of the help that Ad helper components provide is still to be determined, these components have been shown to provide a myriad of functions that are essential for successful AAV replication (Fig. 1-5). The Ad5 E1A and E1b 55k proteins have been reported to perform numerous roles that are essential during AAV gene expression (4). E1A

has a previously well-defined role in the regulation of the expression of the AAV2 P5 and AAV5 P41 promoters; however, the exact role of E1b 55k in AAV replication is not as clear. Ad E2a binds single-strand DNA (ssDNA) and has been shown to function during the strand displacement phase of AAV2 inverted terminal repeat (ITR)-mediated genome replication (4). The E4orf6 protein has been shown to be required for the successful completion of second-strand synthesis; although the mechanism by which it does so is not yet fully understood (9). Previous work done in the Pintel laboratory has shown that while maximal replication of AAV5 requires all five Ad components their combined net enhancement of AAV5 replication is comprised of both positive and negative effects (10). Specifically, although Ad 5 E4orf6 is required for AAV5 genomic replication, it also functions together with E1b 55k to target de novo generated AAV5 small Rep and Cap proteins for ubiquitination and subsequent degradation (10-12). The Ad VA RNA, a small abundantly produced RNA works post-transcriptionally to enhance AAV gene expression at the level of protein translation. VA RNA is not itself translated. It acts as a regulatory RNA during the Ad5 life cycle, and its role in enhancing the translation of Ad5 proteins during infection is well characterized (13). Additionally, it has been shown that mutants of Ad5 VA RNA I that render the RNA deficient in inhibiting the activation and subsequent phosphorylation of protein kinase R (PKR) cannot function as helpers for AAV5 replication (14).

**Figure 1-5 Model of adeno-associated virus (AAV) DNA replication.** The ITR is represented by 5'A'B'C'AD'3' and 5'DA'CBA3'. The various stages of AAV replication are denoted 1 – 7. Briefly, the 3' terminal haripin serves as a primer for DNA synthesis (1, left), or alternatively, the terminal repeat sequence could first base pair to form 'panhandle' (1, right); followed by an elongation step (2); complete copying of the parental strand requires a nick to introduce a new 3'OH (3); elongation from the nick results in the formation of a double-stranded replication intermediate (4); new hairpins are formed (5); a new cycle of DNA synthesis begins (6); followed by strand displacement to release a molecule of single-stranded genomic DNA. The five adenovirus helper components required for AAV replication are shown at various stages in the AAV replication cycle. Adapted from Adapted from S.J. Flint, L.W. Enquist, R.M. Krug, V.R. Rancaniello and A.M. Skalka (ed.), 2009 Principles of Virology, Molecular Biology, Pathogenesis, and ASM Press Washington D.C.

**Figure 1-5 Model of adeno-associated virus (AAV) DNA replication.**

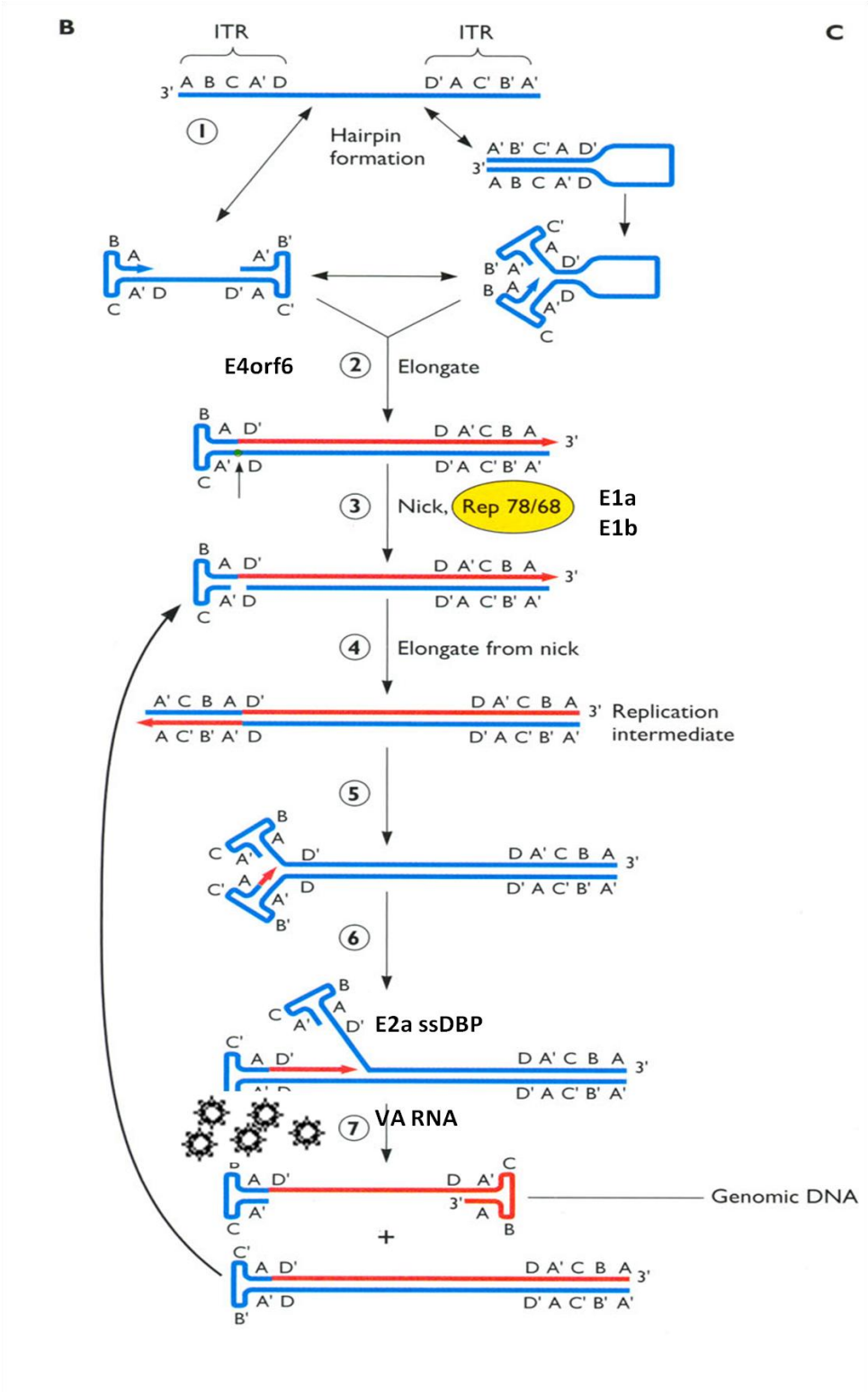

The research summarized in Chapter 2 details results of work done on the ubiquitination and proteasomal degradation of AAV large Rep proteins (Rep 78/68) in the absence or presence of the Ad E1b 55k and E4orf6 proteins. In addition, in collaboration with a previous graduate student, David Farris, we showed that AAV small Rep proteins are ubiquitinated and degraded in a proteasome-dependent manner in the presence of Ad E1b 55k and E4orf6 proteins (12). A more detailed description of the roles these two proteins play in AAV biology is summarized below.

## THE ROLES OF E1B 55K AND E4ORF6 IN AAV BIOLOGY

During AAV replication E4orf6 is required for the second-strand synthesis of nascent ssDNA genomes (Fig. 1-5). Conversion of the ssDNA viral genome into a transcriptionally active double-stranded intermediate is considered to be an important rate-limiting step in the efficient transduction and expression of recombinant AAV vectors and their encoded gene products (9). Additionally, during wild-type Ad/AAV co-infection, the E4orf6 protein is required for head-to-tail concatamerization of AAV genomes, an important process for successful AAV replication (15). It has been hypothesized that a phosphorylated form of the cellular protein FKBP52 (a 52 kDa, FK506-binding protein, also called single-stranded DNA binding protein, ss-DBP) prevents the conversion of AAV ssDNA into the double-stranded replication intermediate (16). Phosphorylated FKBP52 (ss-DBP) binds to the single-strand D –sequence in the AAV2 inverted terminal repeat (ITR) (Fig. 1-6). FKBP52 is phosphorylated at tyrosine residues by the epidermal growth factor receptor protein tyrosine kinase (EFGR-PTK) and de-

phosphorylated by the T-cell protein tyrosine phosphatase (16). During adenovirus co-infection, FKBP52 is de-phosphorylated allowing for the conversion of AAV ssDNA to the double-stranded form (16). Preliminary data from the Pintel laboratory suggests that EGFR-PTK may be a substrate for the Ad E3 ubiquitin ligase which is described in greater detail below (Nayak and Pintel unpublished results).

During viral infection, the Ad5 early proteins, E1b 55k and E4orf6 perform multiple functions at both early and late stages of the viral life cycle. These functions are indispensable for adenovirus replication (17). Early functions include the inactivation of the host-cell protein p53 and prevention of a cellular DNA damage response. Late functions include the simultaneous inhibition of host-cell mRNA export and promotion of viral mRNA export and translation (17).

**Figure 1-6 A possible model for the role of the tyrosine phosphorylated FKBP52 (ssD-BP) in the viral second-strand DNA synthesis and AAV-mediated transgene expression.** The phosphorylated form of ssD-BP preferentially complexes with the D(2) sequence in the AAV ITR and blocks initiation of DNA replication from the 3' OH end. Various indicated conditions or treatments cause dephosphorylation of the ssD-BP, leading to some type of conformational change, which results in accessibility of the 3' OH end as a primer for the second-strand DNA synthesis followed by gene expression. The model is taken from Qing *et al* Proc. Natl. Acad. Sci. USA Vol. 94, September 1997.

**Figure 1-6 A possible model for the role of the tyrosine phosphorylated FKBP52 (ssD-BP) in the viral second-strand DNA synthesis and AAV-mediated transgene expression.**

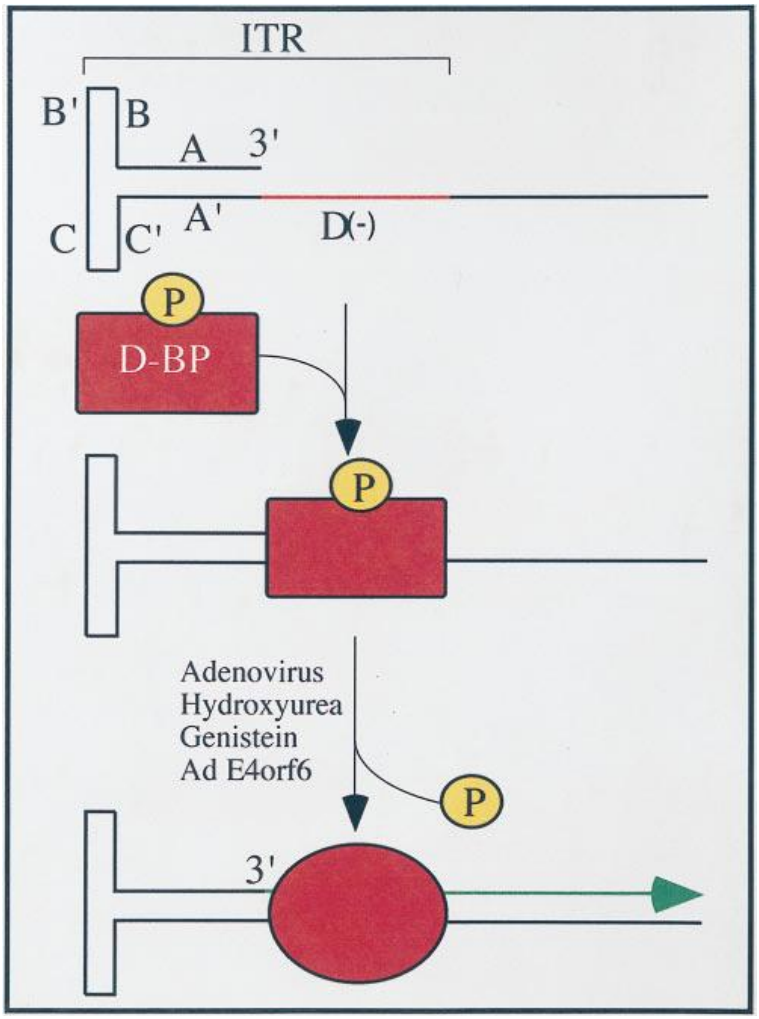

In Ad5-infected cells the E1b 55k and E4orf6 proteins participate in forming an E3 ubiquitin ligase complex (Fig. 1-7) which also consists of the cellular proteins cullin 5 (Cul5), RING-box 1 (Rbx1), and elongins B and C (17). E4orf6 is required to form this complex by interacting with elongin C, while the E1b 55k protein functions as the complex's substrate recognition unit. Previously identified cellular targets of this viral ubiquitin ligase are p53, the MRE11-Rad50-NBS1 (MRN) DNA damage recognition/repair complex, and DNA ligase IV, a protein essential for DNA repair by non-homologous end joining (17). The E1b 55k/E4orf6 ubiquitin ligase also appears to be required for at least some of the late functions of E1b 55k, which involve the inhibition of host cell mRNA export and promotion of late viral mRNA transport from the nucleus. In infected cells, some E1b 55k and E4orf6 proteins accumulate in and around viral DNA replication and RNA transcription sites (17). The complex has also been shown to actively shuttle between the nucleus and cytoplasm (17). Recently, work done in the Pintel laboratory has shown that this Ad E3-Ub-ligase targets AAV small replication and capsid proteins for proteasomal degradation (11). New findings summarized in chapter 2 reveal that AAV2 and AAV5 large replication proteins join a select group of cellular proteins that are targets of this Ad E3-Ub-ligase.

**Figure 1-7 The adenovirus E3 ubiquitin ligase complex (Ad-E3-Ub-ligase).** Ad E1b 55k and E4orf6 proteins form an E3 ubiquitin ligase complex together with cullin 5 and other cellular proteins that target substrates such as p53 for proteasomal degradation. Taken from Blackford and Grand JVI Vol. 83(9) 2009.

**Figure 1- 7 The adenovirus E3 ubiquitin ligase complex (Ad-E3-Ub-ligase).**

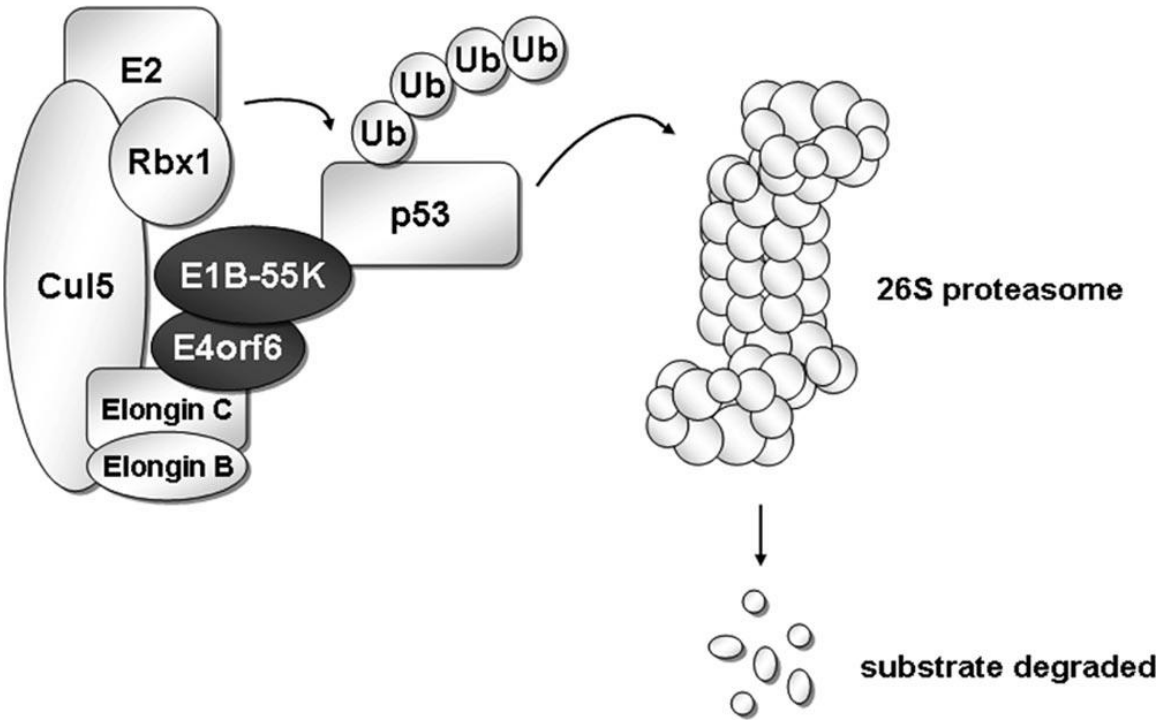

## UBIQUITIN, DIFFERENT FORMS OF PROTEIN UBIQUITINATION AND THE UBIQUITIN PROTEASOME PATHWAY (UPP)

Ubiquitination of proteins represents a key modification that cells employ in order to respond to environmental changes. Ubiquitin (Ub) is a small, highly conserved 76-amino acid, globular protein found in the cytoplasm and nucleus of eukaryotic cells (18). Ubiquitin exists both as a monomer and as isopeptide-linked polymers known as poly-ubiquitin chains. Ubiquitination is achieved by a series of enzymatic reactions where E1, E2, and E3 enzymes conjugate ubiquitin via its C-terminal residue to the ε-amino group of a lysine residue on the target protein (Fig. 1-8). First, the E1 enzyme uses ATP to form a high energy thioester bond between the caboxy-terminus of ubiquitin and an internal cysteine residue in E1. This activated ubiquitin is then transferred to an E2 ubiquitin-conjugating enzyme. Following substrate binding to the E3 ubiquitin ligase, the ubiquitin moiety is transferred to an internal lysine, or in some cases, to the amino terminal amino acid of the bound substrate (Fig. 1-9). The precision of tagging a specific substrate with ubiquitin molecules is achieved by E3 ligases which recognize specific target substrates and mediate the transfer of ubiquitin from an E2 ubiquitin-conjugating enzyme to the substrate. Three classes of E3 enzymes exist: those that contain a HECT domain, a Cullin-RING domain, or a U-box domain (19).

**Figure 1-8 Substrate ubiquitination via E1, E2, and E3 enzymes.** The enzymes that ubiquintate and de-ubiquitinate substrates (S) are indicated, the numbers in parentheses indicate the number of human genes encoding the respective proteins. Taken from The Emerging Complexity of Protein Ubiquitination by David Komander Biochemical Society Transactions (2009) Volume 37, part 5.

**Figure 1-8 Substrate ubiquitination via E1, E2, and E3 enzymes.**

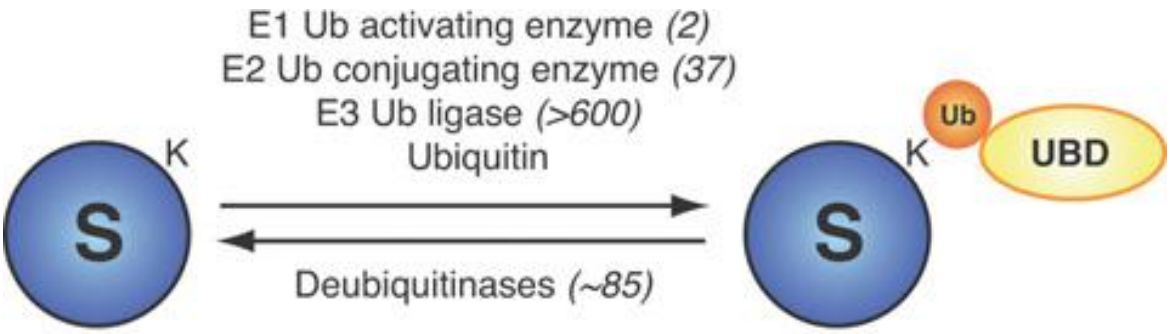

**Figure 1-9 Substrate ubiquitination.** Three types of enzymes: E1, E2, and E3 carry out ubiquitin-modification reactions, including the assembly of polyubiquitin chains (conjugation of additional ubiquitins to a single ubiquitin to form a polyubiquitin chain on some proteins is shown by the brackets in the image). E1s activate ubiquitin so that it is in a reactive state. E2s pick up the ubiquitin from E1 and catalyze the attachment of ubiquitin to the substrate. E3 enzymes, called ubiquitin ligases, are important in substrate recognition and function in concert with E2 to transfer ubiquitin to the substrate. Taken from Origin and function of ubiquitin-like proteins, Mark Hochstrasser Nature 2009 458, 422-429.

**Figure 1-9 Substrate ubiquitination.**

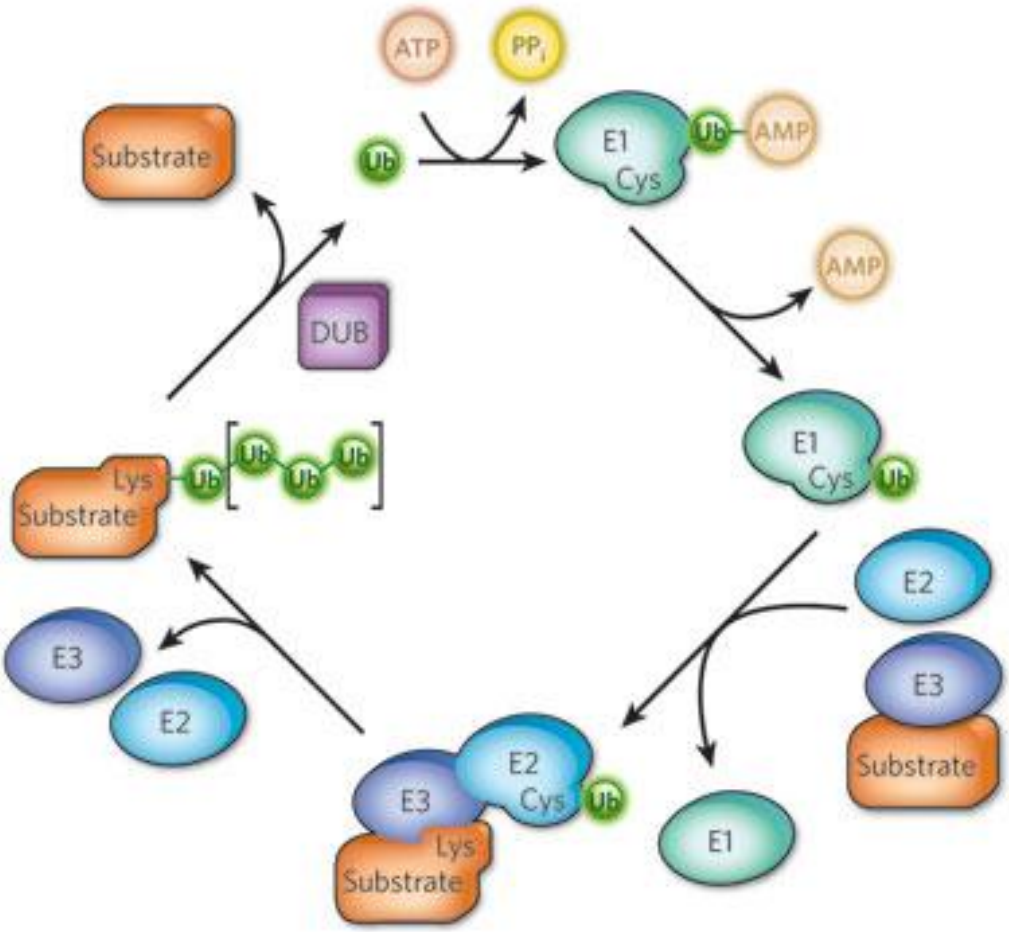

E3 ligases belonging to the HECT domain family contain a C-terminus domain that was first identified in the HPV E6AP protein. This domain binds to the E2 enzyme and contains a conserved Cys residue onto which the activated ubiquitin is transferred. The HECT domain family of E3 enzymes is the only class that first transfers activated ubiquitin to the E3 protein itself prior to transfer to the substrate. The other classes of E3 ligases, one example of which is shown in Fig. 1-7, function more as a scaffold to bring the substrate and the ubiquitin-loaded E2 component together (19) (20).

E3 ligases that belong to the Cullin-RING family contain several ligase complexes that are assembled in a similar manner. Typically, a substrate specificity factor is associated through a linker protein(s) to the amino terminus of a Cullin component, while its carboxy terminus interacts with a RING finger-containing protein (Rbx1 or Rbx2). Recruitment of the E2 conjugating enzyme is carried out by the RING finger protein. Seven human Cullin proteins (Cul1, 2, 3 4A, 4B, 5 and 7) are known to form ligase complexes. These complexes have been called either F-box proteins when assembled with Cul1 or BC-box proteins when assembled with Cul2 or Cul5. The Ad-E3-Ub ligase that is characterized in this study and discussed in chapter 2 contains the Cul5 scaffold protein (Fig. 1-7).

As previously discussed, ubiquitination was first identified as a signal that leads to the degradation of the target protein by the host cell proteasome. Thus, it was thought that this activity is primarily involved in regulating the half-life of target proteins. However, it is now known ubiquitin conjugation can lead to many

different outcomes such as alterations in protein localization, stability or the ability to interact with other proteins depending on the type of ubiquitin attachment as depicted in Fig. 1-10.

The E3 ligases facilitate isopeptide bond formation between ubiquitin and its substrate. The ubiquitin molecule contains seven lysine residues which can serve as acceptors of additional ubiquitin residues thus, adding another element of diversification to the system (Fig. 1-11). Specifically, ubiquitin moieties can be further modified at lysine residues 6, 11, 27, 29, 33, 48 or 63 of the ubiqutin molecule. It has been shown that different ubiquitin linkages can lead to different physiological outcomes for the target protein. Ubiquitin linkages via lysine 48 or lysine 63 have been the most widely studied. Research presented in this thesis (chapter 2) examined whether AAV proteins are modified by lysine 48 or lysine 63 forms of ubiquitination.

**Figure 1-10 Cellular processes that are affected by different types of ubiquitination.** Lys-48-linked chains are most commonly associated with proteasomal degradation, but they can also regulate transcription by a non-proteolytic mechanism. Lys-63 type linkages chains are involved in signal transduction, membrane-protein trafficking, endocytosis and DNA repair. Taken from Origin and function of ubiquitin-like proteins Mark Hochstrasser Nature 2009 458, 422-429.

**Figure 1-10 Cellular processes that are affected by different types of ubiquitination.**

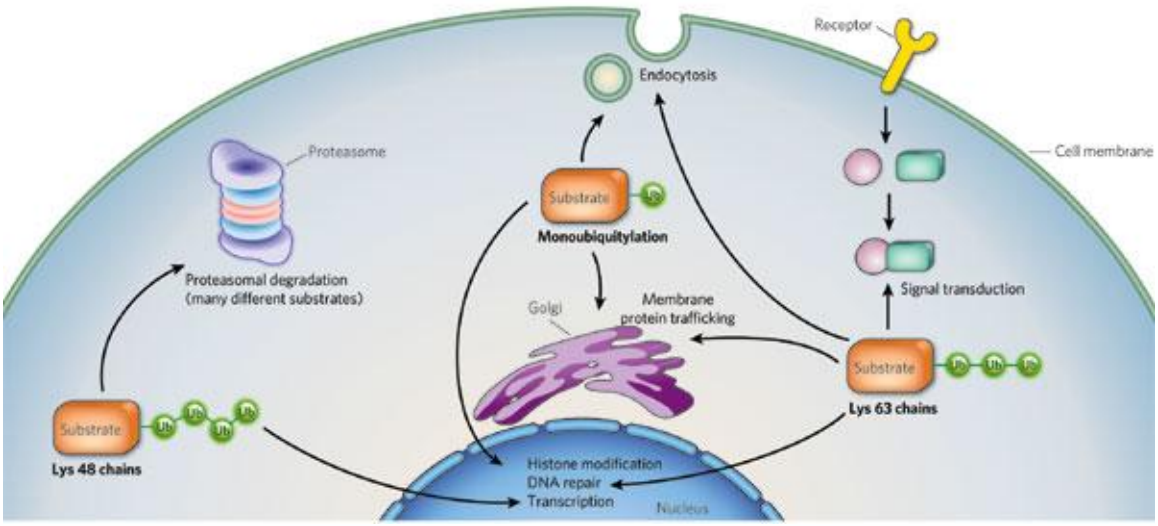

**Figure 1-11 Ubiquitin and its seven lysine residues.** The three dimensional structure of ubiquitin is shown indicating the position of the seven lysine molecules (red) that can be further modified by additional ubiquitination. Shown next to each are the cellular processes that are affected by polyubiquitination at specific lysine residues. Taken from The Emerging Complexity of Protein Ubiquitination by David Komander Biochemical Society Transactions (2009) Volume 37, part 5.

**Figure 1-11 Ubiquitin and its seven lysine residues.**

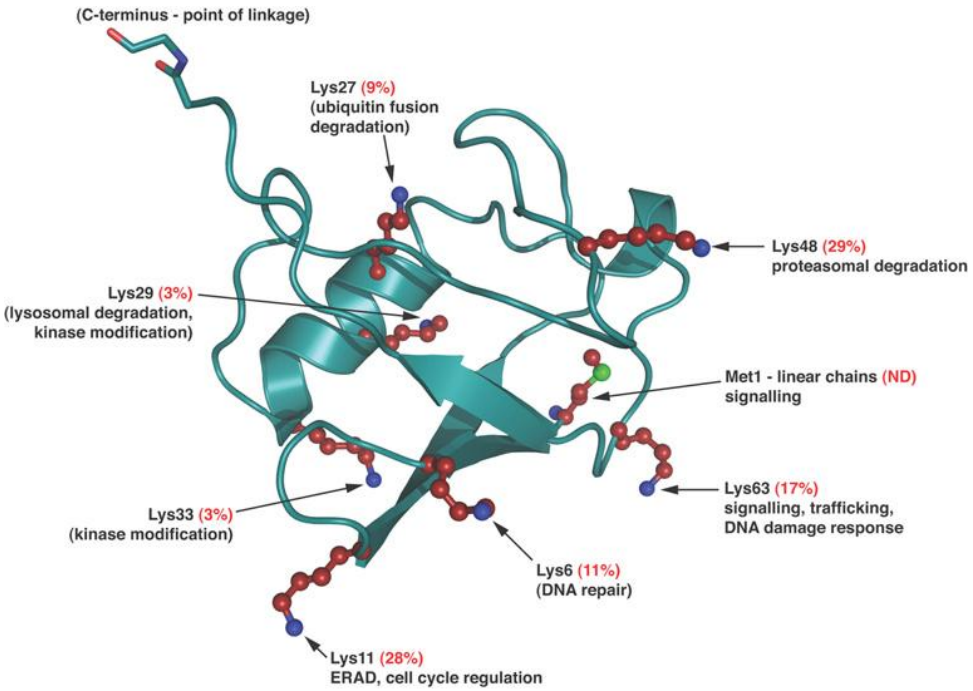

A polymeric chain of ubiquitin residues linked via the lysine 48 sidechain is known to serve as a signal for target proteins to enter the proteasome where they are subsequently degraded. The ubiquitin proteasome pathway (UPP) is discussed in greater detail below. In contrast, extensive research has shown that polyubiquitination at lysine 63 can have non-degradative outcomes particularly among proteins involved in the DNA damage response and cellular signaling (21). Multiple targets of the nuclear factor kappa-B (NF-κB) regulatory pathway are modified by lysine 63 ubquitination and targets within this pathway are generally considered to be the best studied examples of this type of ubiquitin modification (22).

Various substrates that are degraded during the progression of the cell cycle are tagged with lysine 11 forms of ubiquitination (23). Lysine 29 and lysine 33 type linkages are implicated in protein kinase modification. The physiological roles for lysine 27 or lysine 6 chain linkages are unclear although the latter may be involved in DNA repair (23).

Proteins are continually “turning over;” that is; they are being hydrolyzed to their constituent amino acids and replaced by newly synthesized proteins. Protein degradation is as important as synthesis in the maintenance of protein homeostasis in cells. Overall, the rate of protein synthesis and degradation in each cell must be balanced precisely. Cells contain multiple proteolytic systems to carry out the degradation process and complex regulatory mechanisms to ensure that the continual proteolytic processes are highly selective.

The ubiquitin-proteasome pathway (UPP) is the major cytosolic proteolytic system in eukaryotes, with critical functions in cell cycle control, apoptosis, inflammation, signal transduction, protein quality control, and many other biological processes (22). The proteasome, a protease of over 2.5 megadaltons, functions primarily to degrade proteins that have been modified by the attachment of ubiquitin (Fig. 1-12). Abnormalities in ubiquitin-mediated processes have been implicated in many human diseases. As discussed above, ubiquitination is achieved by a series of enzymatic reactions where the enzymes E1, E2, or E3 conjugate ubiquitin via its C terminus to lysine residues in target proteins. Proteins targeted for proteasomal degradation require at least four ubiquitin molecules attached to the Lys-48 residue. The proteasomal-dependent degradation of AAV large replication protein is discussed in more detail in chapter 2.

**Figure 1-12 The ubiquitin-proteasome pathway is responsible for the degradation of a majority of cellular proteins.** A polyubiquitin-modified protein is the form most commonly targeted to the proteasome. Ubiquitin receptors in the proteasome regulatory particle (RP) of the 26S proteasome allow binding of the tagged substrate to the proteasome. ATPases within the RP (shown right) unfold the substrate and translocate it into the 20S proteasome core particle (CP), where the proteolytic sites are located, resulting in the substrate being cleaved. Taken from the article: Origin and function of ubiquitin-like proteins Mark Hochstrasser Nature 2009 458, 422-429.

**Figure 1-12 The ubiquitin-proteasome pathway is responsible for the degradation of a majority of cellular proteins.**

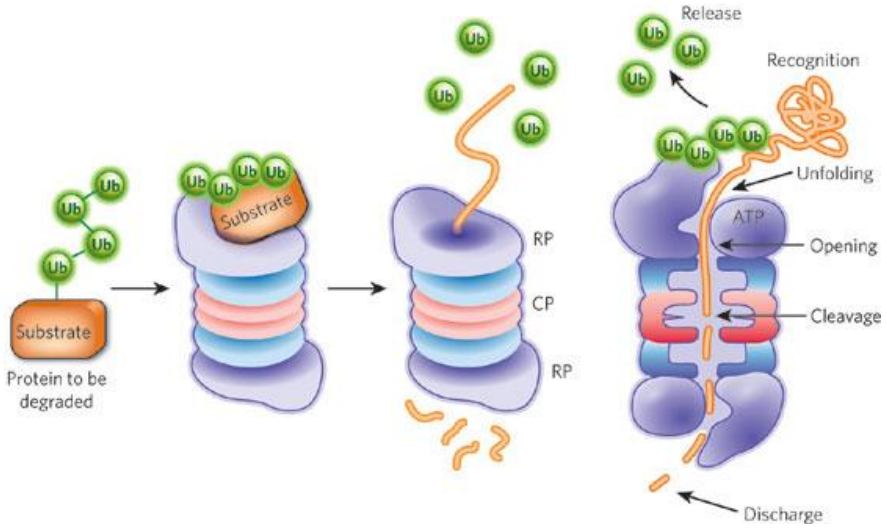

## INTRODUCTION TO BOCAVIRUSES

All bocaviruses are members of the autonomously replicating genera of the sub-family *Parvovirinae* (the parvoviruses) (Fig. 1-1). Similar to other parvoviruses, bocaviruses are small, non-enveloped, single-stranded DNA viruses with icosahedral capsids. The name bocavirus is a composition of the two members initially categorized in this genus, **bo**vine parvovirus (BPV) and minute virus of **ca**nine (MVC), which have a sequence homology of 43%. There are currently three recognized bocavirus members bovine parvovirus type 1 (BPV), minute virus of canine (MVC) and the recently identified human bocavirus (HBoV) (2). Human bocavirus (HBoV) was identified by polymerase chain reaction (PCR) amplification of pooled specimens from small children with respiratory tract infections (24). HBoVs have been reported to be associated with acute respiratory illness and may potentially represent a new human viral pathogen (25). Consequently, there has been a lot of attention given to understanding the biology and pathogenesis of the human bocaviruses. Although an infectious clone for HBoV is available, its characterization has been limited by the lack of a tissue culture system that supports efficient replication (26). However, the related virus, minute virus of canine (MVC) replicates well in tissue culture. MVC causes gastrointestinal and respiratory diseases in neonatal puppies and reproductive disorders in adult dogs (27). The MVC genome has a shared homology of 52.6% and 52.1% with that of the human bocavirus and bovine parvovirus, respectively (28). A phylogenetic map showing the relationships among human bocavirus, bovine parvovirus and the minute virus of

canine is shown in Fig. 1-13. MVC and HBoV also share a high degree of similarity both in the symptoms of diseases they are associated with as well as in the organization of their genomes.

There have been relatively few studies done to understand the biology of bocaviruses. Recent work has shown that MVC induces mitochondrion-mediated apoptosis and G2/M arrest in infected permissive canine cells (29). MVC infection also triggers a DNA damage response resulting in activation of known DNA damage signaling proteins (30). Therefore, a comprehensive characterization of the transcription, translation and replication features of MVC is worthwhile because it not only provides insight into the genus bocavirus but also the data may be relevant to the newly identified HBoV.

**Figure 1-13 Genetic relationships between parvovirus B19, bovine parvovirus, canine minute virus and strains of human bocavirus.**

Phylogenetic tree with 1,000 bootstrap replicates was generated showing the relationship among parvovirus B19, bovine parvovirus, canine minute virus (MVC), and representative strains of human bocavirus (HBoV1-4). Adapted from Xu *et al* PLOS ONE Sep. 2012 Vol. 7 (9)

**Figure 1-13 Genetic relationships between parvovirus B19, bovine parvovirus, canine minute virus and strains of human bocavirus.**

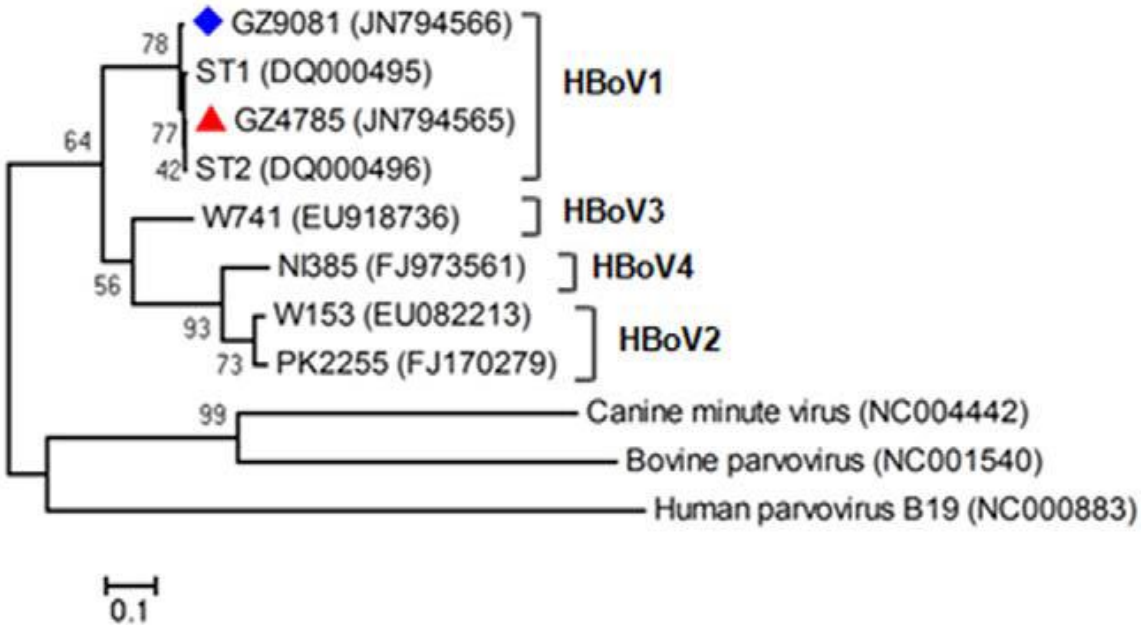

## TRANSCRIPTION PROFILE OF MVC

The MVC genome is 5.4-kilobases in length. The left and right-end termini of the genome are distinct palindromic hairpins of 183 and 198 nt in length, respectively. A fully infectious clone of MVC has been generated and the 5' and 3' terminal palindromes have been sequenced (28). A previously published genetic map of MVC is shown in Fig. 1-14. A single promoter located at map unit 6 (P6) encodes three distinct open reading frames ORFs 1, 2 and 3. An earlier characterization of the genome identified 3 splice donor sites, 1D, 2D, and 3D located at nucleotides 395, 2309 and 3037, respectively. Three splice acceptor sites have also been previously identified, 1A, 2A and 3A located at nucleotides 2199, 2386, and 3037 (28). Through the processes of alternative splicing and alternative polyadenylation, six RNA transcripts are generated that lead to the production of two nonstructural proteins (NS1 and NP1) and two capsid proteins (VP1 and VP2) (Fig. 1-15). Northern blot analyses have revealed that the large non-structural protein NS1 is produced from an un-spliced RNA which is polyadenylated at either a proximal (nt 3258/3288) or distal site (nt 5268) yielding R1 and R2 transcripts, respectively. The NS1 protein with a predicted molecular weight of 85 kDa is indispensable for genome replication (28). The smaller non-structural protein, NP1 is produced from spliced transcripts (spliced at 1D-1A and 2D-2A) that are polyadenylated either proximally or distally. The capsid transcripts (VP1 and VP2) are generated from a spliced product that excises the 1D-1A, 2D-2A and 3D-3A introns or by splicing of the 1D-3A intron. The VP1 and VP2 proteins are 71 and 63 kDa in size, respectively. A third capsid protein, VP3

is generated post-translationally. New research findings that led to a revised transcription map of the MVC genome are described in detail in Chapter three.

There are two additional features of the MVC genome that are noteworthy. The genome contains two identified polyadenylation sites, the proximal site termed (pA)p is located at nucleotide positions 3258/3288 and the distal polyadenylation site (pA)d is located at nucleotide 5268. The proximal polyadenylation site resides within the MVC capsid coding region. Consequently, read-through of the (pA)p site is crucial in order to produce capsid transcripts. Another key feature of MVC is the expression of a 24 kDa non-structural protein, NP1. NP1 is unique to members of the bocavirus genus, and has been shown to be critical for optimal viral replication as mutants of NP1 exhibit severely impaired replication (28). There is a high degree of sequence homology among the NP1 proteins of HoBV, BPV and MVC, however, there is little similarity with other parvovirus proteins or with other known proteins (Fig. 1-16). One of the main foci of our study of MVC is to gain a better understanding of the role(s) this novel NP1 protein play in the MVC life cycle. Our work done on identifying a function for this novel bocavirus protein is presented in Chapter 3.

**Figure 1-14 The genetic map of MVC.** The MVC genome is drawn to scale highlighting the single P6 promoter, the splice donors (D) and acceptors (A), and (pA)p and (pA)d sites. Numbers denote the nucleotide numbers within the MVC genome. The genome encodes 3 distinct open reading frames (ORFs) generating NS1, NP1 and capsid transcripts. Taken from Sun *et al* JVI 2009 83(8) p. 3956-3976.

**Figure 1-14 The genetic map of MVC.**

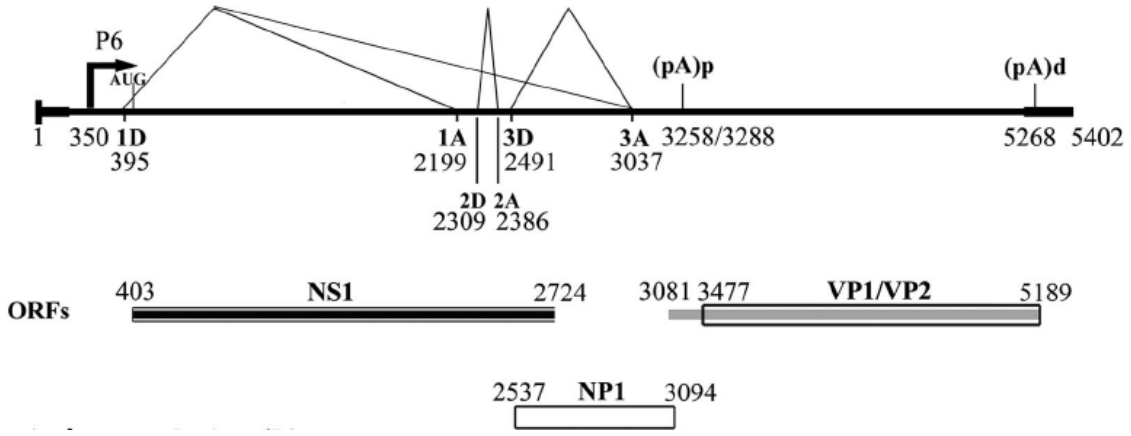

**Figure 1-15 MVC RNA transcripts detected by Northern blot analysis.** The identities and respective sizes (kDa) of the six RNA transcripts in MVC detected by Northern blot analysis are shown on the left and right of the diagram. The large NS1 protein has a predicted molecular weight of 85 kDa (in our studies it is described as an 84 kDa protein). The numbers shown on the far left indicate the relative percentages of the various transcripts as assessed by Northern blot analysis. Taken from Sun *et al* JVI 2009 83(8) p. 3956-3976.

**Figure 1-15 MVC RNA transcripts detected by Northern blot analysis.**

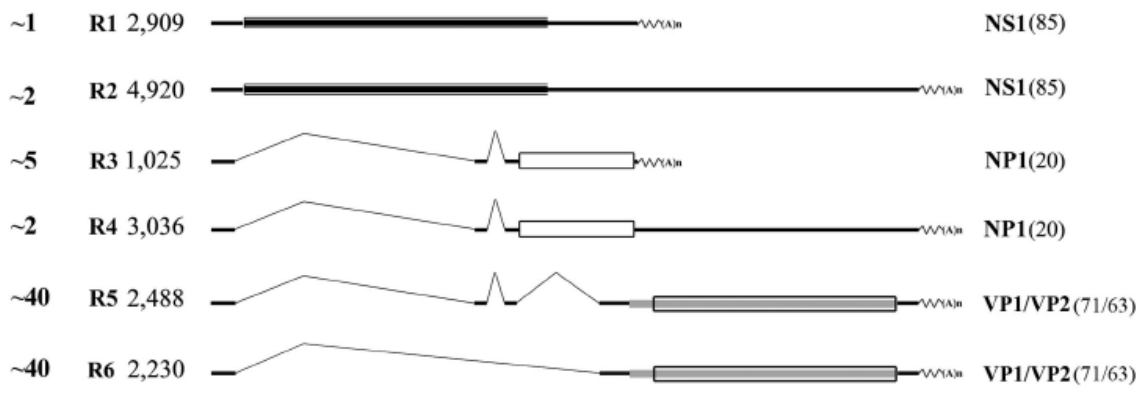

**Figure 1-16 Phylogenetic analysis of bocaviruses NP-1 sequences.** The NP1major open reading frame was analyzed on the basis of both nucleotide (top) and protein (bottom) sequences of representative variants of human bocavirus (HBoV1, empty; HBoV, filled circles, MVC (empty rectangle), and bovine parvovirus 1 (filled rectangle). Adapted from Kapoor *et al* JID 2009: 199(2).

**Figure 1-16 Phylogenetic analysis of bocaviruses NP-1 sequences.**

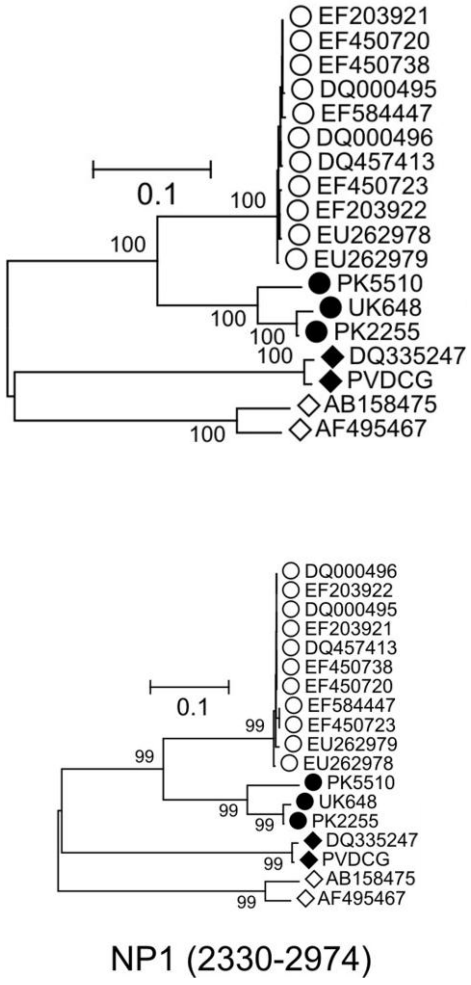

## PARVOVIRUS RNA PROCESSING STRATEGIES TO ACCESS CAPSID TRANSCRIPTS

Due to their compact genomes parvoviruses utilize a number of different strategies to maximize gene expression. RNA processing strategies including transcriptional regulation, alternative splicing, and alternative polyadenylation are key mechanisms among the arsenal of tools that these viruses employ to expand and regulate gene expression. Other processes in RNA biogenesis such as those involved in regulating RNA export are also exploited as a means of modulating gene expression (31). In addition, parvoviruses also use post-translational modifications to control gene expression (32).

To achieve productive infection, parvoviruses must accumulate proper levels of capsid protein. Capsid protein production is considered to be a rate-limiting step for the amplification of single-stranded genomic DNA and subsequent virion production. Appropriate levels of capsid expression can be attained by a number of mechanisms. Parvoviruses with multiple promoters such as MVM or AAV2 encode a capsid-specific promoter to generate capsid transcripts. Furthermore, these viruses also ensure maximal capsid transcription by transactivating the capsid promoter via the actions of their large non-structural proteins.

The MVM genome is organized into two overlapping transcription units with promoters at map units 4 (P4) and 38 (P38) (Fig. 1-17). The P4 promoter generates RNA species R1 and R2 which encode the non-structural proteins NS1 and NS2, respectively. The P38 promoter generates R3 RNAs that encode

the viral capsid proteins VP1 and VP2. The MVM NS1 protein provides multiple functions that are important in the viral life cycle. One of the key functions of NS1 is to transactivate the P38 promoter (33). Studies aimed at understanding the transactivation properties of NS1 have shown that the C-terminal region of NS1 alone is sufficient for transactivation of the capsid promoter (34). Overall these studies show that MVM uses its NS1 protein to regulate capsid gene transcription.

Similar to MVM, the AAV2 genome is also arranged into two overlapping reading frames encoding non-structural and capsid proteins (Fig. 1-18). The non-structural gene transcripts are produced from one of two promoters located at map positions 5 (P5) and 19 (P19), and an internal splice donor and acceptor site. Transcription of the non-structural genes generate four transcripts that are translated into four replication proteins: Rep78, Rep68, Rep52 and Rep40 the nomenclature of which is based on the relative molecular weights of the protein products.

The capsid gene is transcribed from a single promoter at map position 40 (P40). Two capsid transcripts encoding virion proteins 1 and 2 (VP1 and VP2) are generated via alternative splicing at two acceptor sites. A third virion protein (VP3) is generated from a downstream AUG within the VP2 transcript. AAV2 large Rep protein transactivates the P40 capsid promoter in a manner that requires binding to the transcription template at either the ITR or the P5 promoter (35). This process has been reported to work in part by stabilizing a loop-like structure that localizes the P5 promoter and its cognate transcription factors to

the P40 promoter (35). The transactivation potency of the large Rep protein is greatly enhanced by co-infection with adenovirus (35).

**Figure 1-17 Genetic map of MVM.** The three major transcript classes (R1, R2, R3) are shown relative to the 5 kb genome diagrammed below. The proteins that they encode are listed on the right of each transcript, and the open reading frames (ORFs) used for each are indicated. The locations of the promoters (P4 and P38) are indicated. The large intron is excised using a non-consensus donor (ncD), and a poor polypyrimidine tract ([Py]n) at its 3' splice site. The different ORFs that are used are shown in different shading patterns. Taken from PARVOVIRUSES (Hodder Arnold 2006) Chapter 18, Parvovrius RNA processing strategies by Jianming Qiu, Yuko Yoto, Gregory Tullis and David J Pintel.

**Figure 1-17 Genetic map of MVM.**

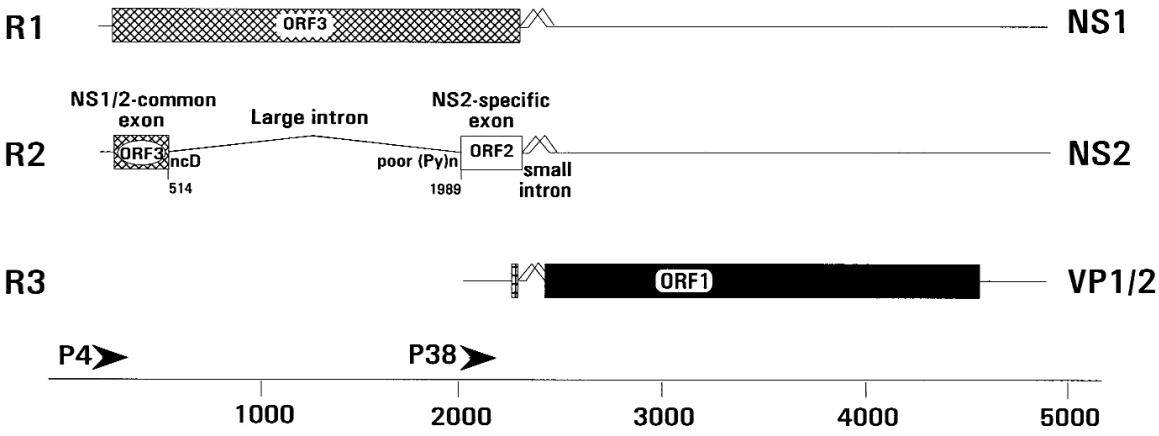

**Figure 1-18 Transcription profile of AAV2.** The transcription map of AAV2 depicting the P5, P19, and P40 promoters, spice donor (D) and acceptors (A1, A2). Numbers denote the nucleotide numbers in the AAV2 genome. RNA species transcribed from each of the promoters is shown. Adapted from PARVOVIRUSES (Hodder Arnold 2006) Chapter 18, Parvovrius RNA processing strategies by Jianming Qiu, Yuko Yoto, Gregory Tullis and David J Pintel.

**Figure 1-18 Transcription profile of AAV2.**

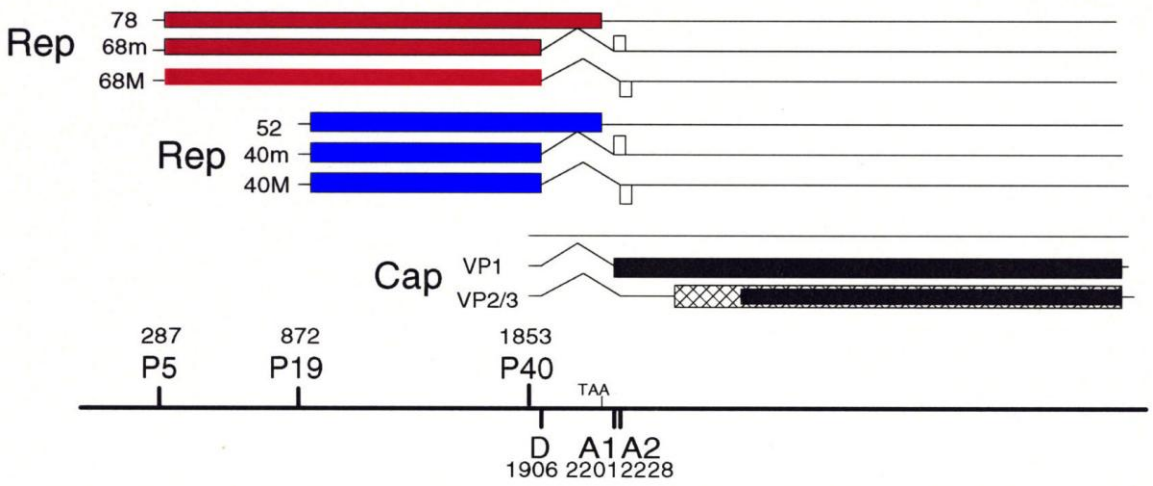

The genomes of parvoviruses such as the erythrovirus, amdovirus and bocavirus genera encode a single promoter, a fact which requires them to utilize complex post-transcriptional processing strategies for capsid production. Consequently, for these viruses, capsid protein production is an important element governing their replication strategies. All members of these genera encode a proximal, (pA)p and a distal (pA)d polyadenylation sites. The (pA)p site is further distinguished by its location within the viral genome; it can be located either within an intronic region as is the case for the erythroviruses or within a coding region as seen in the bocaviruses and amdoviruses.

B19, the prototypical virus of the erythrovirus genus, is the only parvovirus known to be pathogenic in humans. B19 causes a number of diseases including fifth disease in children, arthropathy, particularly in women, and hydrops fetalis following infection of the fetus in utero (36). The transcription map of B19 is shown in Fig. 1-19. A single pre-mRNA is transcribed from the single promoter located at map unit 6 (P6), and at least twelve RNA transcripts are generated via the processes of alternative splicing and alternative polyadenylation (37). There are two polyadenylation sites, one at the distal end, (pA)d and the other located at the proximal site, (pA)p. Furthermore, two internal (pA)p sites have also been identified, (pA)p1 and (pA)p2 (37). Polyadenylation of B19 pre-mRNAs at the major proximal site, (pA)p1, is governed by a non-consensus core cleavage and polyadenylation specificity factor-binding hexanucleotide, AUUAAA (A sequence). The additional (pA)p site, (pA)p2, with a consensus hexanucleotide sequence AAUAAC (B sequence), lies 296

nucleotides downstream of (pA)p1. Both polyadenylation sites have been shown to be used following B19 infection and transfection of permissive cells with a genomic clone (37). RNAs polyadenylated at (pA)p2 comprise approximately 10% of B19 RNAs that are polyadenylated at the proximal site (37). Mutations within the A and B sequences abolish RNAs polyadenylated at (pA)p while mutations of the B sequence result in a small increase in internal polyadenylation at (pA)p1 (37). However, mutations of the A sequence result in a significant reduction of RNAs that are polyadenylated at (pA)p1 suggesting that the A sequence is the core element necessary for polyadenylation at the (pA)p1 site (37). Additionally, genetic studies have shown that a 50 nt downstream element (DSE) and a 22 nt upstream element (USE) as well the B sequence influence the efficient use of the (pA)p1 site (37). The rates of alternative polyadenylation and alternative splicing are key features that determine the relative amounts of the B19 non-structural and capsid proteins and this balance strongly influence the tissue-specific replication of the B19 virus (38). Recent studies have shown that in the absence of viral replication the majority of B19 transcripts are polyadenylated at the (pA)p site in both permissive and non-permissive cells (39). However, under conditions where the B19 genome can replicate there is an increased read-through of the (pA)p site thereby increasing the proportion of RNAs that polyadenylate at the (pA)d site relative to the (pA)p site (39). As discussed earlier, these date reinforce the concept that the complex relationship between alternative splicing and alternative polyadenylation can influence the type and amount of specific RNA transcripts necessary for virion production.

The B19 viral genome has two introns as shown in Fig. 1-19. Transcripts utilize either splice donor 1 (D1) to splice acceptor 1 (A1-1 or A1-2) or splice donor 2 (D2) to splice acceptor 2 (A2-1or A2-2). The proximal polyadenylation site, (pA)p is located within the second intron, between D2 and A2-1. It has been shown that mutations within the first intron result in a significant reduction in transcripts polyadenylated at the (pA)p site (38). Furthermore, abrogation in splicing of the second intron results in preferential polyadenylation at the (pA)p site. On the other hand, improved splicing from the second intron reduces the relative amounts of transcripts that are polyadenylated at the (pA)p site (38). Conversely, genetic modifications that enhance polyadenylation at the (pA)p site result in a reduction in transcripts spliced at the D2 site (38). All of these results require a replication competent genome as inhibition of viral replication results in preferential polyadenylation at the proximal (pA)p site. Collectively, these results suggest that splicing of the B19 virus pre-mRNA within the second intron influences the choice of polyadenylation sites thereby regulating capsid protein production and that this is a determining factor in efficient progeny production.

**Figure 1-19 Transcription map of parvovirus B19.** The viral genome is depicted and includes the location of the viral promoter (P6), the donors and acceptors, the polyadenylation sites (pA)p and (pA)d, and the terminal repeats (TR). The major transcript classes, their size in nucleotides, and the proteins that they encode are shown below. Open reading frames (ORFs) used to encode the viral proteins are shown above the genome. Taken from PARVOVIRUSES (Hodder Arnold 2006) Chapter 18, Parvovrius RNA processing strategies by Jianming Qiu, Yuko Yoto, Gregory Tullis and David J Pintel.

**Figure 1-19 Transcription map of parvovirus B19.**

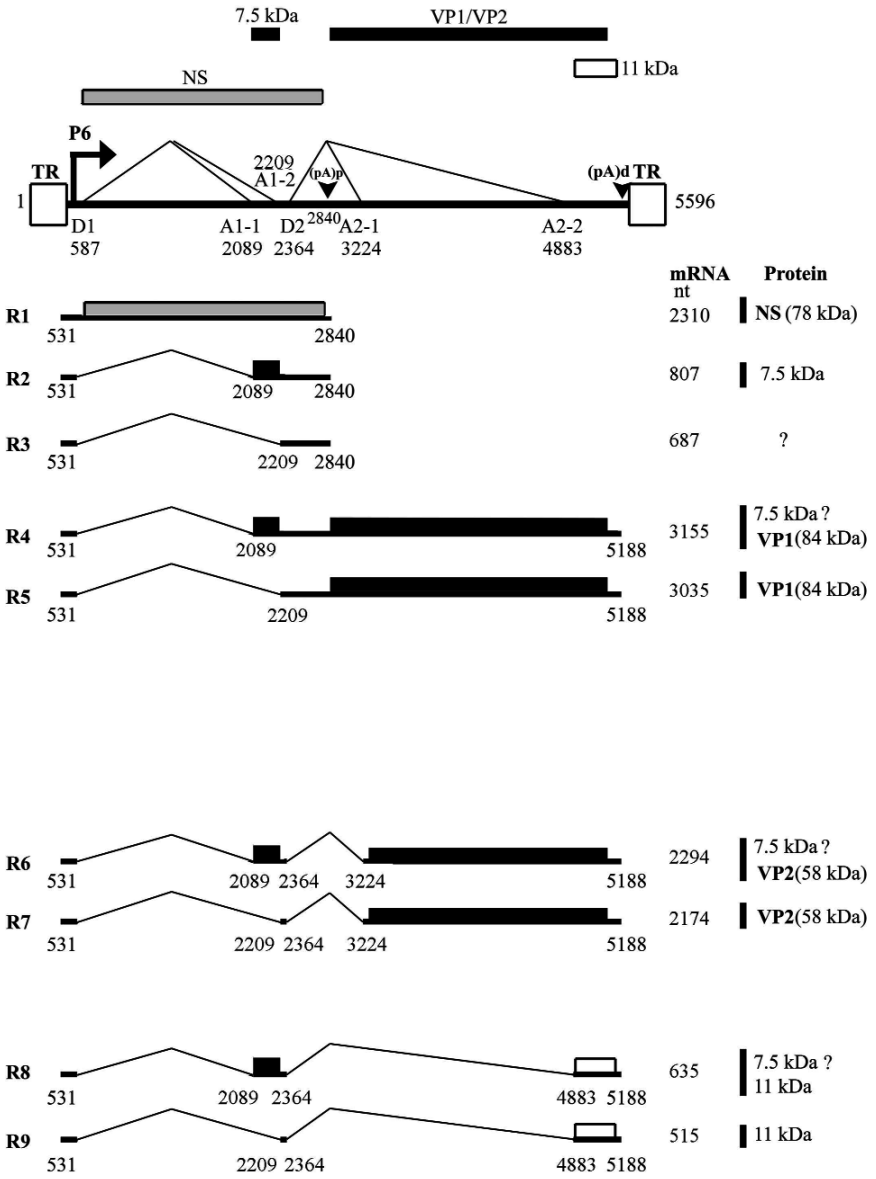

As described in detail in Chapter 3, in contrast to the B19 virus, our work indicates that the regulation of polyadenylation signaling in the bocavirus MVC is independent of genome replication. Moreover, MVC also uses a novel approach to regulate capsid protein expression involving the NP1 protein.

Work done in the Pintel lab has previously shown that Aleutian mink disease virus (AMDV) capsid proteins are cleaved by capsase 10 and this event may play a role in regulating progeny virus production as cleaved capsids lead to a significantly lower number of infectious progeny. AMDV, the only species in the amdovirus genus, causes a persistent infection and severe dysfunction of the immune system in adult minks (40). A transcriptional map of AMDV is depicted in Fig. 1-20. Capsid cleavage may allow the virus a means of maintaining long-term persistence (41). More recently, it has been shown that cis elements located 200 nt upstream (USE) and 40 nt downstream (DSE) of a canonical core cleavage and polyadenylation specificity factor-binding hexanucleotide site (AAUAAA) and the site itself can have an effect on relative capsid production (39). Mutations in the entire 200 nt USE, the AAUAAA site, or the 40 nt DSE which do not affect the amino acid sequence but prevent proximal polyadenylation lead to an increase in capsid protein expression, resulting in a 2-3 fold increase in virion production. These data suggested that AMDV regulation of the proximal (pA)p site may be used as a strategy to modulate capsid protein expression (39). The research presented in Chapter 3 outlines a novel way by which the bocavirus MVC permits read-through of its internal polyadenylation site in order to access caspid transcripts necessary for efficient production of progeny.

**Figure 1-20 The transcription map of AMDV.** The transcription map of AMDV highlighting the P3 promoter, splice junctions, donor (D) and acceptor (A) sites, (pA)p and (pA)d sites are shown by arrows and the splice junctions by thin lines. The P36 promoter is described in an earlier characterization and is depicted as a gray arrow to indicate that its presence is not confirmed by experiments described in this reference. Numbers denote the nucleotide numbers in the AMDV genome. TR denotes inverted hairpin terminus. Taken from Qiu *et al* JVI 2006 p. 654-662.

**Figure 1-20 The transcription map of AMDV.**

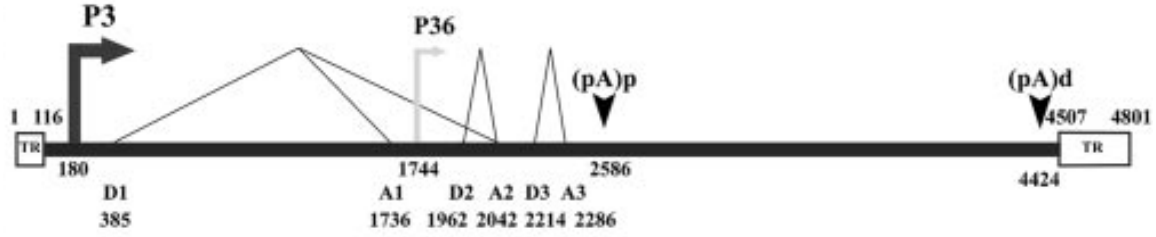

# CHAPTER II

# THE LARGE REP PROTEIN OF ADENO-ASSOCIATED VIRUS TYPE 2 (AAV2) IS POLYUBIQUITINATED

**ABSTRACT**

Five adenovirus gene products are required for efficient replication of co-infecting adeno-associated virus; however, the combined net enhancement by these factors is composed of both positive and negative effects. Similar to previous results with AAV Rep52, AAV2 large Rep was targeted for ubiquitination and degradation by the Ad E4orf6/E1b 55k, cullin 5-containing, E3-ubiquitin ligase. Additionally, large Rep was targeted for ubiquitination via extension of ubiquitin lysine K48 and K63 both in the presence and absence of E4orf6.

## INTRODUCTION

Adeno-associated viruses are members of the Dependovirus genus within the *Parvoviridae* virus family (42). AAV can only achieve efficient productive replication in the presence of a larger helper virus (43). Adenovirus and herpes simplex virus (HSV) are two common helper viruses that support AAV replication (43-44).

The individual helper activities for Ad products essential for AAV2 replication have been extensively characterized (42-44). They include the Ad early gene products E1a, E1b 55k, E4orf6, the single-stranded DNA-binding protein E2a, and VA RNA; however, their combined net enhancement on AAV5 replication is comprised of both positive and negative effects (10). Previous work done in our laboratory has shown that although Ad 5 E4orf6 is required for AAV5 genomic DNA replication, it also functions together with E1b 55k to target de novo generated AAV5 small Rep and Cap proteins for ubiquitination and subsequent degradation (10-11). This targeted degradation of AAV small Rep and Cap was mediated by an E3 ubiquitin-ligase that included Ad E4orf6/E1b 55k, together with Cullin 5 and elongins B and C (11). Degradation of the AAV5 proteins was inhibited by a dominant-negative ubiquitin and by siRNA directed against cullin 5 (11). The Ad E3 ubiquitin ligase, comprised of E4orf6, E1b 55k, elongins B and C, and cullin 5 (Ad-E3 Ub-ligase) had previously been characterized for its role in regulating p53 function and stability as part of an important strategy Ad uses to ensure efficient viral replication (17, 19, 45-47). Thus, the degradation of de novo-generated AAV5 small Rep and capsid proteins joined a select group of

proteins targeted by the Ad-E3 Ub-ligase. Additionally, we have shown that the AAV5 small Rep protein exhibits both K48 and K63 forms of ubiquitination (48). Polyubiquitination of small Rep proteins via lysine K48 linkages, normally associated with targeting of proteins for proteasomal degradation, was detected only in the presence of E4orf6. E4orf6/E1b 55k-dependent K48-specific polyubiquitination of small Rep proteins could be inhibited using siRNA to cullin 5 (48).

AAV2 large Rep proteins (Rep 78/68), in the presence of a helper virus, provide a myriad of functions that are essential for AAV replication (43-44). Large Rep provide site specific endonuclease and helicase activities that are critical for AAV DNA replication, significantly activates AAV promoters for transcription, is involved in alternative splicing of viral RNA, packaging of the virus and site-specific integration of viral DNA into human chromosome 19 (49-56). AAV large Rep can interfere with Ad replication and can have profound effects on cellular metabolism (57-60). Importantly, little is known about how the AAV large Rep protein is modified post translationally in vivo.

## MATERIALS AND METHODS

**Plasmid Constructs.** N/terminal tagged AAV2 and AAV5. The polymerase chain reaction was used to construct hemagglutinin (HA) epitope tagged versions of AAV2 and AAV5. PCR fragments of the N/t HA tagged AAV2 large Rep was cloned in an HIV expressing vector and the N/t HA tagged AAV5 large Rep was cloned in a pcDNA3.1 expressing vector. Detection of N/t HA tagged AAV2 or AAV5 large Rep protein was done by in vitro transfection of the respective plasmids into 293 cells and expression determined by immunoblotting. A monoclonal anti-HA antibody (cat# H9658; Sigma) was used to detect the HA-tagged Rep proteins and monoclonal antibodies 7B73.2 or 303.9 were used to verify AAV2 or AAV5 large Rep proteins, respectively. Additional constructs used in these experiments were as follows: myc tagged or HA tagged E4orf6, a dominant negative ubiquitin construct (UBR7) and a Flag tagged E1b 55k. An anti-HA antibody (cat# H9658; Sigma) was used to detect HA tagged E4orf6.

**Infection and transfection.** Transfections were performed in 293 cells using Lipofectamine Plus (Invitrogen, CA). Co-transfections were done at a 1:1 mass ratio. MG132 (Calbiochem cat# 474791, 10 uM) was added during the last 6 hrs. of the experiment. AAV infections were done in the presence of adenovirus at an MOI of 10.

**Ubiquitination experiments:** In vitro ubiquitiantion: AAV Rep-specific ubiquitination was determined by co-transfection of an HA tagged Rep and a Flag tagged ubiquitin with or without the adenovirus E4-orf6 (myc tagged).

Plasmid DNA (3 ug total per 6-well dish or 6 ug total per 60 mm dish) were transfected into 293 cells using either Lipofectamine Plus or PEI transfection reagents. Co-transfections of plasmids expressing AAV HA-tagged Rep, Flag tagged ubiquitin and myc tagged E4orf6 were done at a 1:1:1 mass ratio. Approximately 36 hours post-transfection, cells were treated with the proteasome inhibitor MG-132 or DMSO (control) for 6 hrs. Cells were pelleted, extracted with RIPA buffer and lysates were blocked with protein G beads for 1 hr. Following blocking, lysates were then incubated overnight with an anti-HA monoclonal antibody at 4 degrees with rocking. Following incubation with the primary antibody, the lysates were pulled down with ProteinG, washed and lysed with Lameilli buffer. The lysates were subjected to immunoblot analysis using a monoclonal anti-7B73.2 or 303.9 antibodies to detect to detect AAV2 and AAV5 large rep proteins, respectively. An anti-Flag monoclonal antibody (cat# F3165; Sigma) was used to detect ubiquitinated Rep proteins.

K-48 or K-63 specific ubiquitination: Mutant forms of HA tagged ubiquitin that allowed extension only on K48 or K63 were transfected in 293 cells instead of a plasmid expressing Flag tagged ubiquitin as described above. An anti-HA antibody (cat# H9658; Sigma) was used to detect ubiqutinated large Rep proteins.

In vivo ubiquitination: 293 cells were infected with AAV/Ad for 24 hrs, with MG132 added during the last 6 hrs. Cell lysates were immunoprecipitated with anti-large Rep 7B73.1 antibody followed western blotting with an anti-ubiquitin

antibody (cat #SC-8017; Santa Cruz Biotechnology to detect endogenous antibody.

**siRNA knockdown of Cullin 5.** 293 cells were transfected with either siRNAs to cullin 5 (cat# GS8065; Qiagen) or scrambled siRNAs serving as negative controls. These transfections were done twice, at the time of plating and 18 hrs. later. Six hours following the second siRNA delivery, cells were transfected with constructs expressing HIV LTR-driven HA-tagged large Rep, HA-tagged K48 ubiquitin and E4orf6. MG132 or DMSO vehicle controls were added during the last six hours of the experiment. Thirty-six hours later cell lysates were immunoprecipitated with an anti-7B73.1 large Rep antibody followed by immuno-blotting with an anti-HA antibody to detect specific K48 ubiqutination of large Rep. Specific knockdown of cullin 5 was accessed by western blotting of equivalent amounts of pre-immunoprecipitation samples. Pre-immunoprecipitation samples were measured for protein content by a spectrophotometer at 595 nm wavelength using the Bradford reagent.

**Large rep/E1b 55k co-immunoprecipitation.** 293 cells were transfected with plasmids expressing HIV LTR driven HA tagged large Rep, Flag tagged E1b 55k and myc-tagged E4orf6. Cell lysates were immunoprecipitated with an anti-E1b 55k antibody (gift of A. J. Berk, UCLA), followed by immunoblotting using the 7B73.2 anti-large Rep antibody. Extracts were prepared under non-denaturing conditions and processed as previously described (48) with one modification: interfering IgG chains were stripped from the immunoprecipitation elution using

the ExactaCruz reagent (Santa Cruz Biotechnology cat# SC-45042) in order to visualize the E1b 55k protein.

## RESULTS AND DISCUSSION

In this study, we show that the Ad E3 Ub-ligase also targets AAV large Rep proteins (Rep 78/68) for ubiqutination and subsequent ubiquitination-dependent proteasomal degradation following AAV2-Ad5 co-infection and during transient transfection. The large Rep proteins exhibited both K48-linked and K63-linked types of polyubiquitination; however, in contrast to previous results with Rep 52, for which only K63-linked polyubiquitination could be detected in the absence of E4orf6 (48), both K48 and K63 types of large Rep ubiquitination were detected in either the presence or absence of E4orf6. Large Rep proteins could be found in complexes with E1b 55k, and levels of Rep K48 ubiquitination were decreased following siRNA knockdown of cullin 5. Although its role in infection is not yet understood, the ubiquitination and potential accelerated proteasomal degradation of AAV large Rep proteins, particularly in the presence of Ad E4orf6 (and E1b 55k), may represent important events in the AAV life cycle.

### AAV LARGE REP IS DEGRADED IN THE PRESENCE OF AD E4ORF6 AND E1B 55K AND IS MODIFIED BY UBIQUITINATION.

We have previously shown that the Ad helper functions required for AAV replication provide a surprising combination of positively and negatively acting effects, and the Ad E4orf6/E1b 55k E3-ubiquitin ligase (Ad E3 Ub-ligase) can target both AAV Rep52/40 and AAV capsid proteins for ubiquitination and subsequent degradation (10-11). The role during infection for this activity is not yet fully understood. Steady-state levels of AAV protein are not seen to be reduced during co-infection with Ad, or when supported by the full panoply of Ad helper functions, because enhancement of AAV mRNA translation by Ad VA

RNA restores AAV protein to levels required for efficient infection (14). Because the AAV large Rep protein is the major viral protein required for genome replication, and because it shares approximately 2/3 of its amino acid sequence with the targeted smaller Rep proteins, we sought to determine if the large Rep protein were also a target of the Ad E4orf6/E1b 55k E3 Ub-ligase. It has previously been shown that when expressed alone in cells, large Rep is a stable protein exhibiting a long half-life, similar to AAV/Ad co-infection. Therefore, as seen previously during our analysis of Ad effects on AAV Rep 52/40 and Cap (11), we expected that Ad E3 Ub-ligase-targeting of Rep for degradation would be only clearly apparent in the absence of VA RNA.

As can be seen in Fig. 2-1A, accumulated levels of the large Rep protein expressed in Ad E1a- and E1b-expressing 293 cells are significantly reduced in the presence of Ad E4orf6 (compare lanes 1 and 2). Additionally, large Rep levels can be recovered in the presence of the proteasome inhibitor MG132 (Fig. 2-1A, lane 3), suggesting that the E4orf6-dependent degradation of large Rep is proteasome mediated. In these experiments, 293 cells were transfected with a HIV LTR-driven HA-tagged large Rep-expressing plasmid, either with or without HA-tagged E4orf6. 36 hrs later samples were prepared for immunoblotting as previously described (48), using anti-Rep78/68 monoclonal 7B73.2 (61) to detect large Rep, and anti-HA antibody to detect E4orf6. MG132 was added during the last 6 hours to samples as indicated. Ad E4orf6 mutants previously described (10), which are deficient in Ad E3 Ub-ligase formation and hence incapable of causing targeted ubiquitination were unable to cause a reduction in accumulated

Rep levels (data not shown). Taken together, these results suggest that the Ad E4orf6/E1b 55k E3 Ub-ligase targets AAV large Rep for proteasomal degradation, and thus, large Rep joins p53, Mre11, DNA ligase IV, integrin $\alpha$3, and AAV small Rep and Cap proteins as part of a select group of proteins targeted by this ligase complex (11, 45, 47, 62-67).

**Figure 2-1 AAV large Rep proteins have reduced stability in the presence of Ad E1b 55k/E4orf6 and are modified by ubiquitination.** A. Immunoblots of samples taken from 293 cells transfected with HIV LTR-driven HA-tagged Rep in the absence (lane 1) or presence or HA-tagged E4orf6 (lanes 2 and 3) as described in the text. Transfections treated with MG132 are shown in lane 3. Tubulin was used as a control for the amount of protein loaded per lane. Rep was detected using anti-Rep78/68 monoclonal 7B73.2 (61), E4orf6 was detected with anti-HA antibody, and tubulin with anti-tubulin. B. Immunoblots of extracts from mock infected (lane1), AAV alone infected (lane 2), Ad alone infected (lane 3), AAV/Ad infected (lane 4), or AAV/Ad infected with MG132 (10uM) added, immunoprecitpitated with anti Rep 7B73.2 and subsequently immunoblotted with anti ubiquitin antibody. C. Immunoblots of extracts taken 48 hrs following transfection of 293 cells with HIV LTR-driven HA-tagged AAV2 Rep (left panel), CMV-driven AAV5 Rep (right panel), Flag-tagged ubiquitin, and HA-tagged E4orf6 as indicated and described in the text, either in the presence or absence of MG132 as shown. Ubiquitinated Rep was detected with anti-Flag antibody. D. Immunoblots of extracts taken 48 hrs following transfection of 293 cells with HIV LTR-driven HA-tagged AAV2 Rep, a plasmid expressing HA-tagged ubiquitin allowing extension only on K48 (left panel), a plasmid expressing HA-tagged ubiquitin allowing extension only on K63 (right panel), and E4orf6 as indicated and described in the text, either in the presence or absence of MG132 as shown. Cell lysates were immunoprecipitated with an anti Rep 7B73.2 and subsequently

immunoblotted with anti ubiquitin antibody. Ubiquitinated Rep was detected with anti-HA antibody.

**Figure 2-1 AAV large Rep proteins have reduced stability in the presence of Ad E1b 55k/E4orf6 and are modified by ubiquitination.**

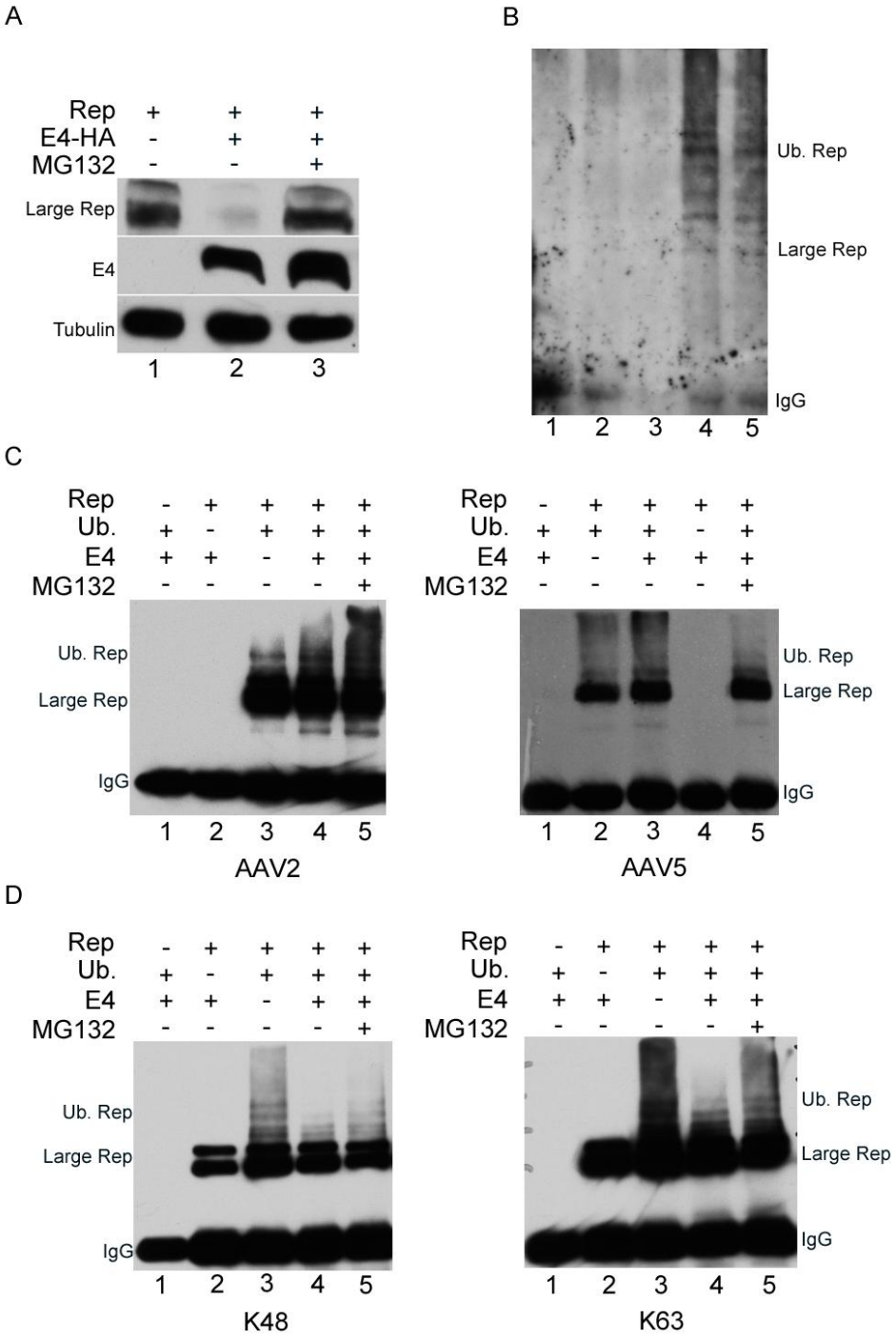

If Rep is a target of the Ad E3 Ub-ligase, we should be able to demonstrate ubiquitination of Rep during AAV/Ad co-infection. As can be seen in Fig. 2-1B, during AAV2/Ad5 co-infection, immunoblots of large Rep immunoprecipitated with the anti-Rep78/68 monoclonal 7B73.2 (61) and probed with an anti-ubiquitin antibody revealed high molecular weight ubiquitin conjugates of Rep both in the presence and absence of MG132 (Fig.2-1B, lanes 4 and 5). Extracts from mock infected cells, or cells infected with either AAV or Ad alone showed no specific ubiquitination reactivity (Fig. 2-1B, lanes 1-3). These experiments were done under stringent washing conditions that we have previously shown fully dissociate cellular proteins, including any potentially Rep-associated, ubiquitinated proteins, from our immunoprecipitates (48).

To further characterize the ubiquitination of large Rep, we developed a ubiquitination assay utilizing transiently expressed HIV LTR-driven HA-tagged Rep and Flag-tagged ubiquitin. Ubiquitination of both AAV5 and AAV2 large Rep were assayed in 293T cells both in the presence and absence of added E4orf6. In these assays, large Rep was immunoprecipitated using the 7B73.2 antibody, and equivalent amounts of sample were immunoblotted with anti-Flag antibody to detect specific ubiqitination, as previously described (48). As expected, both AAV2 (left panel) and AAV5 (right panel) large Reps were ubiquitinated in the presence of E4orf6, which in 293 cells would reconstitute the Ad E3-Ub ligase (Fig. 2-1C, left panel lane 4, and right panel lane 3), but surprisingly, significant ubiquitination of Rep was also detected in the absence of E4orf6 (Fig. 2-1C, left panel lane 3, right panel lane 2). The addition of MG132 had little effect in these

experiments (Fig. 2-1C, left and right panel, lanes 5), likely because the immunoprecipitations were sub-quantitative (data not shown).

## THE AAV SMALL REP PROTEIN IS ALSO MODIFIED BY POLYUBIQUITINATION.

During the studies above examining the ubiquitination of AAV2 large Rep proteins a collaboration was established with Dr. David Farris while he was a graduate student in the Pintel laboratory. These studies were designed to determine if the AAV2 small Rep protein is also modified by ubiquitination. The results shown in Fig. 2-2 demonstrate that in E1b positive 293T cells, plasmid-expressed AAV2 small Rep is ubiquitinated in both the presence and absence of the Ad E4orf6 protein. This collaboration lead to a *Journal of Virology* publication in which I was a coauthor (48).

**Figure 2-2 AAV2 small Rep protein is polyubiquitinated.** Top panel. Extracts from 293T cells co-transfected with plasmids expressing HA-small Rep (Rep), Flag-tagged ubiquitin (Ub) and myc-tagged E4orf6 (E4). The extracts were immunoprecipitated with an antibody against HA and then subjected to immunoblot analysis with an antibody against Flag. Lanes (1) Ub + E4 (2) Rep + E4 (3) Rep + Ub (4) Rep + Ub + E4 (5) Rep + Ub + E4 + MG132. Bottom panel. Expression of AAV2 small Rep was confirmed by immunoblot analysis of extracts from 293T cells co-transfected with plasmids described in the top panel. This blot was probed with a monoclonal antibody specific for HA.

**Figure 2-2 AAV2 small Rep protein is polyubiquitinated.**

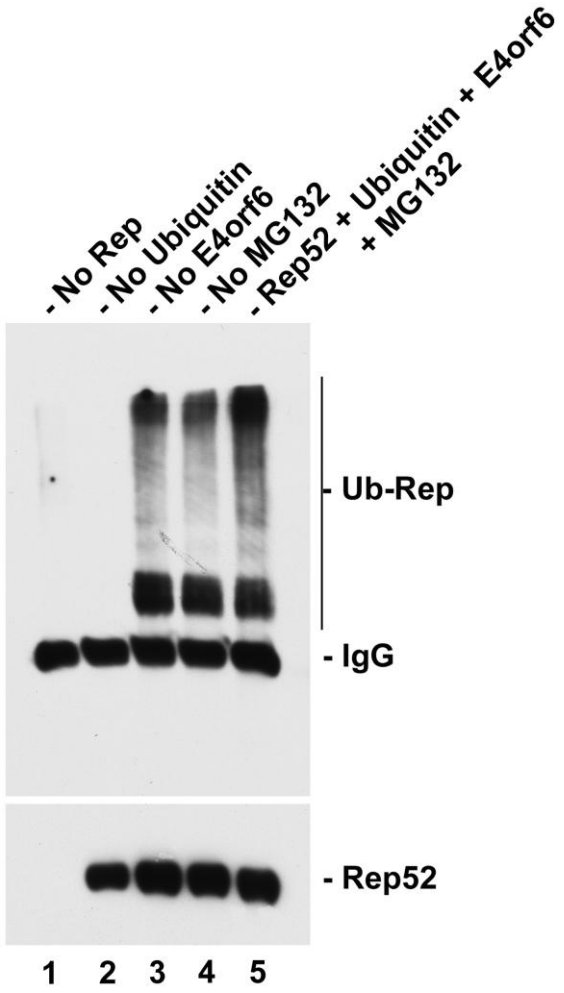

**AAV LARGE REP IS UBIQUITINATED VIA K48 AND K63 EXTENSION BOTH IN THE PRESENCE AND ABSENCE OF E4ORF6.**

There are multiple types of ubiquitination. Polyubiquitination that extends through lysine 48 of ubiquitin is most-often associated with proteasomal degradation (68-69). The other major form of ubiqutination, extending ubiquitin lysine 63, is most often associated with other modifications of protein function (20). We have previously reported that AAV5 Rep52 is ubiquitinated using both K48 and K63 polyubiquitination (48). One possibility that might explain both E4orf6-dependent and E4orf6-independent ubiquitination of large Rep would be that different forms of ubiquitin were added under these different conditions. To further characterize the ubiquitination of large Rep, we used transient expression assays, similar to those described above, and as previously described (48), in which mutant forms of HA-tagged ubiquitin that allowed extension only via K48, or alternatively only via K63 (70-73), were supplied in trans.

Fig. 2-1D demonstrates that large Rep undergoes both the K48-extension (left panel) and K63-extension (right panel) form of polyubqiuitination. However, surprisingly, both types of ubiquitination were found both in the presence of Ad E4orf6 (Fig. 2-1D, left and right panel, lanes 4 & 5), and in its absence (Fig. 2-1D, left and right panels, lane 3). These results suggest that the targeting of large Rep for both K48 and K63 ubiquitination can be accomplished by factors other than the Ad E3 Ub-ligase. Ubiquitination patterns were not detected in cell extracts from transfections lacking either Rep or HA-ubiquitin (lanes 1 & 2, left and right panels), or in which an HA-tagged ubiquitin that allowed extension only on K29 was included (data not shown).

**THE AD E3 UB-LIGASE PARTICIPATES IN THE UBIQUITINATION AND DEGRADATION OF AAV LARGE REP.**

Although we have demonstrated that large Rep can be ubiquitinated via K48 and K63 extension both in the presence and absence of Ad E4orf6, ubiquitination by the Ad E3 Ub-ligase must be an important feature of Ad/AAV interaction because, as shown in Fig. 2-1A, ubiquitin-targeted degradation of large Rep is dependent on the E4orf6/E1b 55k Ad E3 Ub-ligase. To demonstrate this involvement more directly, we examined the E4orf6-dependent ubiquitination and targeted degradation of Rep in the presence of the dominant-negative ubiquitin, UBR7 (74), as previously described (11). As can be seen in Fig. 2-3, both the E4orf6-dependent ubiquitination (Fig. 2-3A, compare lane 3 and 4 to lane 5), and the targeting of large Rep for degradation (Fig. 2-3B, compare lane 2 to lane 3), was suppressed by the addition of a dominant-negative ubiquitin, implicating the Ad E3-Ub-ligase in this process. For experiments shown in Fig. 2-3A, 48 hrs post-transfection of 293T cells HIV LTR-driven HA-tagged Rep was immunoprecipitated with antibody 7B73.2, and immunoblotted with either anti-Flag (Fig. 2-3A, top panel) or anti-7B73.2 Rep (Fig. 2-3A, bottom panel) to detect Flag-tagged ubiquitin, or large Rep, respectively. For experiments shown in Fig. 2-3B, 293 cells were transfected with HIV LTR-driven HA-tagged Rep either alone, or together with E4orf6, or E4orf 6 plus UBR7, as indicated. Expression of HA-tagged E4orf6 was confirmed with an anti-HA antibody (Fig. 2-3B, bottom panel). In Fig. 2-3A, substantial levels of Rep remain even in the presence of E4orf6 (lane 3 bottom panel) because these immunoprecipitations are sub-quantitative (data not shown). We have previously shown that the Ad E3 Ub-

ligase targeted loss of AAV Rep52 evident by Western blotting was not apparent following sub-quantitative immunoprecipitation of Rep (48).

**Figure 2-3 E4orf6 dependent-ubiqutination and degradation of AAV large Rep is suppressed by the addition of a dominant negative ubiquitin.** A. Immunoblots of large Rep immunoprecipitated with 7B73.2 and immunoblotted with anti-Flag (top panel) or anti-Rep (7B73.2) (bottom panel) in the presence or absence of the dominant negative UBR7 or MG132 as indicated, and as described in the text. B. Immunoblot of samples taken from 293 cells transfected with HIV LTR-driven HA-tagged large Rep alone (lane 1), or with co-expression of E4orf6 (lane 2), or E4orf6 together with UBR7 (lane 3). Large Rep was detected with 7B73.2 and E4orf6 expression was detected by HA (lower panel). Cellular tubulin was used as a loading control.

**Figure 2-3 E4orf6 dependent-ubiqutination and degradation of AAV large Rep is suppressed by the addition of a dominant negative ubiquitin.**

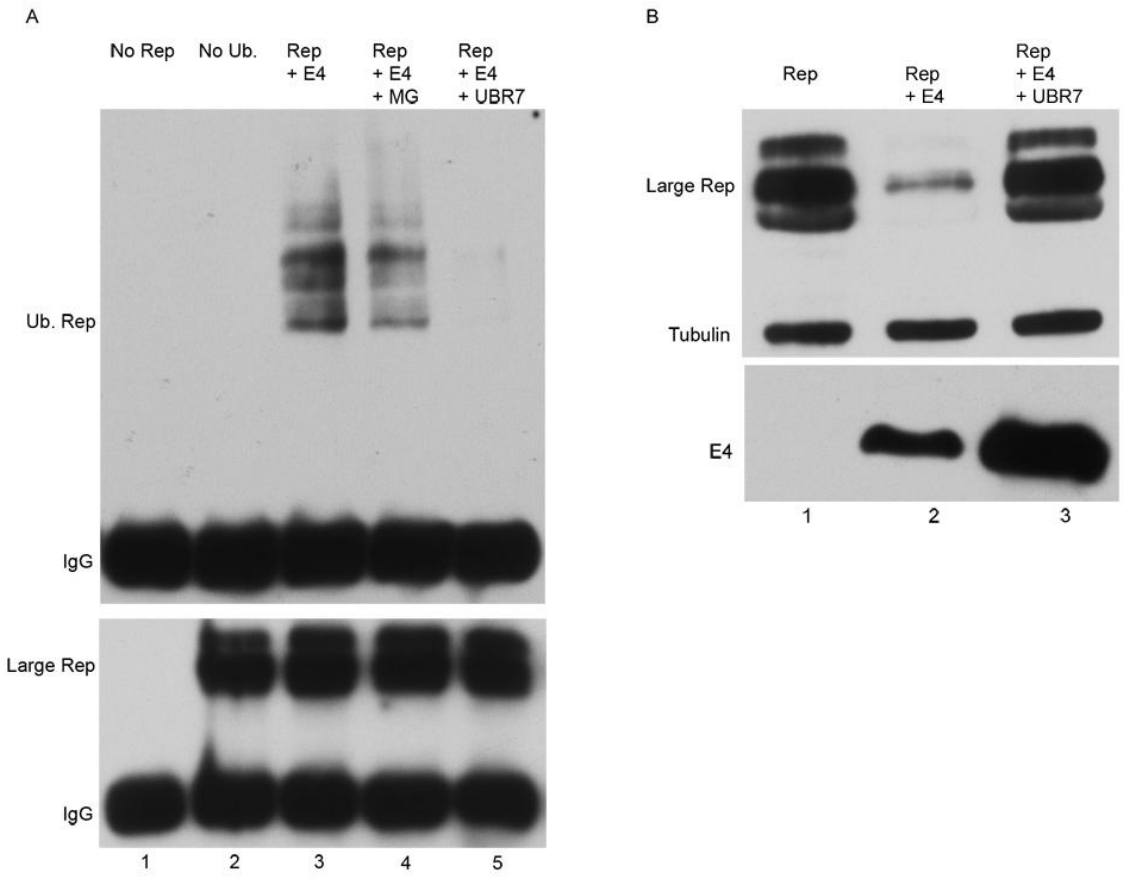

Consistent with the involvement of the Ad E3-Ub-ligase in these processes, siRNA-mediated knockdown performed exactly as previously described (48) (and detailed in the Materials and Methods) of cullin 5, the cullin present in the Ad E3-Ub-ligase, dramatically reduced E4orf6 –dependent (and to a much lesser extent E4orf6-independent) K48 ubiquitination of large Rep (Fig. 2-4A, compare lanes 9 and 10 to 5 and 6).

Additionally, in the presence of control siRNA, the activated form of cullin 5 apparent as the higher migrating species of cullin 5 (75) was seen only in the presence of E4orf6 (Fig. 2-4A, compare lanes 1, 2, 5 & 6 with lanes 3 & 4). This is consistent with cullin 5 participating in the Ad E3-Ub-ligase targeted ubiquitination of Rep, but not in the ubiquitination of Rep in the absence of this ligase described above.

**Figure 2-4 The Ad E3 Ub-ligase participates in the ubiquitination and degradation of AAV large Rep.** A. Top panel: Immunoblots of extracts taken 36 hrs following transfection of 293T cells with HIV LTR-driven HA-tagged AAV2 Rep, an HA-tagged ubitquitin allowing extension only on K48, and E4orf6 as indicated and described in the text, either in the presence or absence of MG132 as shown. In addition, either siRNAs directed toward cullin 5 (Cul5, lanes 7-10), or scrambled control siRNAs (lanes 1-6) were added as described in the text. Ubiquitinated Rep was detected with anti-HA antibody. Bottom panel: Pre-IP western blot of the same samples in the top panel probed with anti-cullin 5 antibody to monitor specific knockdown of cullin 5. Cellular tubulin was detected as a marker for the amount of protein present in each sample. B. Immunoblot of cell lysates transfected with plasmids expressing E1b 55k, large Rep or E4orf6 as indicated. Following transfection, lysates were immunoprecipitated under non-denaturing conditions with an anti-E1b 55k antibody, followed by western blotting with an anti-large Rep antibody 7B73.2. The lower panel shows the same samples probed with an anti-E1b 55k antibody to demonstrate the presence of E1b 55k. A slower migrating non-specific band is observed in all lanes as denoted by an asterisk.

**Figure 2-4 The Ad E3 Ub-ligase participates in the ubiquitination and degradation of AAV large Rep.**

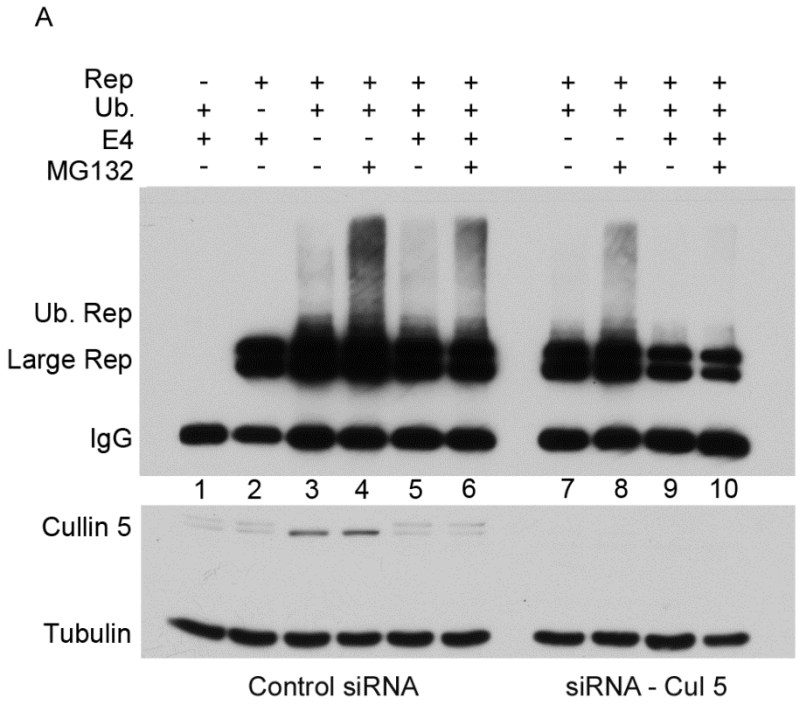


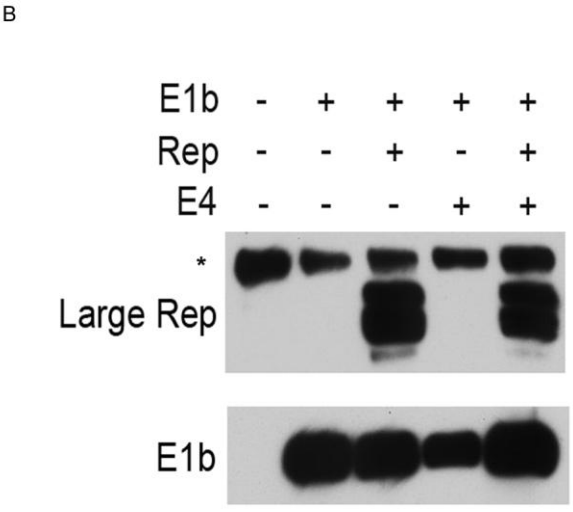

We next sought to begin to identify components that could comprise the complex(es) that direct the ubiquitination of large Rep. As can be seen in Fig. 2-4B, immunoprecipitation with an anti-E1b 55k antibody, followed by immunoblotting using the 7B73.2 anti-large Rep antibody, demonstrated that in 293 cells large Rep and E1b 55k form a stable complex both in the presence and absence of E4orf6. This interaction has been reported previously by others as well as ourselves (11, 51). These results suggest a role for this interaction other than as part of the Ad E3 Ub-ligase, and further suggest that within the Ad E3 Ub-ligase complex the E1b 55k protein may interact directly with large Rep irrespective of the presence of E4orf6. Although the full nature of the roles that the individual helper functions play during AAV infection is not yet fully understood, the Ad E3-Ub-ligase-targeted ubiquitination and proteasomal degradation of AAV large Rep proteins may represent important events in the AAV life cycle.

# CHAPTER III

# CHARACTERIZATION OF THE NON-STRUCTURAL PROTEINS OF THE BOCAVIRUS MINUTE VIRUS OF CANINE (MVC)

## AUTHOR'S NOTE

The work presented in Chapter 3 represents a collaboration between myself and my colleague Olufemi Fasina. On the submitted manuscript reporting this work currently undergoing peer review, we are credited equally as co-first authors. Many of the experiments described in this chapter involved multiple steps to which we contributed equally. The manuscript also included contributions from our co-authors Lisa Burger and Ayushi Rai. Therefore it is difficult to separate and attribute specific individual contributions in each of the experiments detailed in this chapter. Thus, the reader should understand that the work presented in Chapter 3 was a collaborative effort.

In an effort to denote specific contributions from each author I have tried to assign the major contributor of each of the figures. However, as noted above each of the co-first authors share equal credit. Fig.3-1A left panel (LS), Fig.3-1A middle panel (LS, OF), Fig.3-1A right panel (LS), Fig.3-1B (LS), Fig.3-1C (LS), Fig.3-2A left panel (LS), Fig.3-2 middle panel (OF), Fig.3-3 right panel (OF), Fig.3-2B (LS, OF), Fig.3-3A (LS, OF), Fig.3-3B (LS, OF, LB, AY), Fig.3-3C (LS,OF,LB), Fig.3-3D (OF), Fig.3-3E (LS, OF), Fig.3-3F (LS, OF), Fig.3-3G (LS, OF), Fig.3-3H (LS), Fig.4 (LS).

**ABSTRACT**

We present a detailed characterization of a single cycle infection of the bocavirus minute virus of canines in canine WRD cells. This has allowed identification of an additional smaller NS protein that derives from an mRNA spliced within the NS gene that had not been previously reported. In addition, we have identified a role for the viral NP1 protein during infection. NP1 is required for read-through of the MVC internal polyadenylation site and thus access of the capsid gene by MVC mRNAs. Although the mechanism of NP1's action has not yet been fully elucidated, it represents the first parvovirus protein to be implicated directly in viral RNA processing.

## INTRODUCTION

The Bocavirus genus of the Parvovirus family has gained renewed interest recently because of the identification of a bocavirus of humans (HBoV) that has been associated with lower-respiratory tract infections in children (2, 76). Although an infectious clone of HBoV has recently been reported, characterization of this virus has previously been limited by the lack of a robust tissue culture system that supports efficient replication (77).

We have chosen to more fully characterize the bocavirus of canines (MVC) as a prototype of the bocavirus genus. This virus, isolated many years ago (27, 78-79), features an efficient tissue culture system; an infectious clone has been constructed that replicates well following transfection of permissive cells; and we have developed accurate traditional plaque assays and plaque-lift assays for titering virus.

The general transcription maps for MVC, HBoV, and a third bocavirus, bovine parvovirus (BPV), have been delineated and have been found to be similar (28, 77, 80). They feature a single promoter at the left hand end of the genome which generates multiple mRNAs that are derived from a single pre-mRNA by alternative splicing and alternative polyadenylation at either a proximal (pA)p or distal (pA)d site (see Fig.3A). The proximal polyadenylation signal must be suppressed for viral RNAs to extend into the right-hand end of the genome and access the capsid-coding region. This signal must be retained during export to the cytoplasm and remain in these mRNAs throughout their existence. Another important novel feature of the bocaviruses is the presence of the viral

NP1 protein (28, 81). This abundantly produced protein has no homologue in parvoviruses of other genera (82). The BPV life-cycle has been examined in a general way previously (28, 81), and more recently, an examination of the cellular DNA-damage response to MVC infection has been reported (29-30).

In this manuscript we present the results of a detailed examination of MVC infection of canine cells. We describe basic features of MVC single-cycle infection, including a kinetic analysis of viral products and analysis of viral protein stability and localization. We have identified an additional smaller NS protein that derives from an mRNA spliced within the NS gene that had not been previously reported. In addition, we have identified a role for the viral NP1 protein in RNA processing. This is the first parvovirus protein to be associated with such a role.

## MATERIALS AND METHODS

**Viruses and cells.** The minute virus of canine (MVC) virus used in this study was the original strain (GA3) isolated from lung tissue(78) and was kindly provided by Dr. Colin Parrish at Cornell University. It was grown in the WRD cell line (79) through two passages (MVC GA3 P2). A fully infectious wild-type MVC infectious clone (WT IC) was constructed as previously described by Jianming Qiu at the University of Kansas (28). Plaque assays and plaque lift assays were developed to titer virus. All cells were maintained in Dulbecco's modified Eagle's medium with 10% fetal calf serum in 5% CO2 at 37°C.

**Infection and transfection.** For single cycle infections, WRD cells were para-synchronized by isoleucine deprivation as described (33), followed by MVC infection (MOI = 10); re-infection was blocked by the addition of a neutralizing anti-MVC antibody two hours after the initial MVC infection. The neutralizing MVC antibodies from naturally infected canines were provided by Dr. Colin Parrish. Transfections were performed with WRD or 293T cells using either Lipofectamine Plus (Invitrogen, CA) or LipoD293 transfection reagent (SignaGen Laboratories, MD) according to the manufacturer's instructions.

**Antibodies.** Polyclonal anti-NS1 or anti-NP1 antibodies were produced by immunizing rabbits (New Zealand whites – SPF) on day 0 followed by two boosts with either NS1 or NP1 specific peptides coupled to KLH. Two distinct anti-NS1 antibodies were generated against NS1 epitopes targeting either the N-terminus amino acids 30-40 (anti-NS1 NH2) or the C- terminus amino acids 687-700 (anti-

NS1 COOH) of the NS1 protein. A peptide consisting of amino acids 1-13 of the NP1 protein was used as the immunogen to produce anti-NP1 antibodies. Anti-capsid antibodies produced in rabbits were kindly provided by Dr. Colin Parrish. Additional antibodies used in this study were purchased from commercial sources.

**Cycloheximide experiments.** The stability of NS1 and NP1 proteins was accessed by cycloheximide (CHX) inhibition of newly synthesized proteins and performed as described previously (11). Briefly, WRD cells were plated in six-well dishes to 60 - 70% confluence and then infected with MVC at an MOI of 10. At 30 h post-infection, CHX (Sigma Chemicals, MO) was added to the cells at 100 µg/ml. Control wells received dimethyl sulfoxide vehicle instead of CHX. Cells were then collected at the time points described in the text and subjected to immunoblot analysis as described.

**SDS-PAGE, Immunoblot, and Immunofluorescence assays.** SDS-PAGE, Western blotting, and immunofluorescence assays were performed as previously described (31). For immunofluorescence, para-synchronized WRD cells were grown on glass coverslips in 24-well plates and infected with MVC at an MOI of 10. After 18 hrs, cells were washed with PBS, fixed with 4% paraformaldehyde for 15 min and extracted with 0.5% Triton X-100 in PBS for 10 min. Nuclei were visualized by staining with DAPI (49,69-diaminido-2-phenylindole). The coverslips were mounted in Fluoromount-G (Southern Biotech) and light microscopy images were taken at a magnification of 200 or 400x (objective lens)

with an Olympus IX-70 inverted fluorescence microscope. Anti-NS1 or anti-NP polyclonal rabbit antibodies raised against specific epitopes as described above were used at 1/1000 dilution followed by incubation with a goat anti-rabbit IgG conjugated with FITC (Sigma). DAPI was utilized as a nuclear counterstain.

**Southern blotting.** WRD cells were transfected with the MVC constructs as described in the text and figure legends. At 48 hours post-transfection, DNA was extracted from transfected cells and DNA replication was accessed by Southern blotting as described previously (83) using whole MVC genome probes derived by Not1 digestion of the full length MVC WT IC. A one kilobase fragment from the MVM capsid region was inserted into the plasmid backbone to clearly separate input plasmid from the monomer RF. Loading of samples was normalized using a nanodrop spectrophotometer.

**Plasmid constructs.** Multiple constructs were used in this study as described below.

***MVC pIMVC.*** The MVC wild-type infectious clone was generated as previously described (28).

***NS1 (full length)/pcDNA3.1.*** MVC NS1 was constructed by inserting MVC NS1 ORF with additional flanking sequences (nt 340 to 2750 of the MVC pIMVC) into pcDNA3.1.

***NS1 mutant infectious clone.*** The NS1 ORF was terminated by introducing a TAG stop codon at nt 416 with a single T insertion in the MVC IC.

***Spliced NS1/pcDNA3.1.*** The NS1 spliced cDNA was generated by reverse transcription and cloned into pcDNA (Invitrogen, CA).

***NP1 (full length)/pcDNA3.1.*** MVC NP1 was constructed by inserting MVC NS1 ORF (nt 2537 to 3096) into pcDNA3.1.

***NP1 pre-mature termination mutants.*** The NP1 ORF was terminated by introducing a TAG stop codon at nt 2735 with a single T mutation in MVC IC using overlapping PCR techniques. Additional NP1 pre-mature termination mutants were made by converting either nt 2738-2740 or nt 2837-2839 to TAA using site-directed mutagenesis.

***NP1-ATGm.*** The NP1 initiating codon was mutated at nt 2537 from AUG to GCG.

***NP1-5XPro.*** This mutant was made by introducing 5 prolines in a row starting at nt 2780 in the MVC IC.

***NP1 Capsid Fusion mutant.*** An NP1 mutant was made by a single nt deletion at nt 3089 resulting in a fusion of the NP1 and Capsid ORFs.

***3A splice acceptor mutant.*** A 3Am mutant was constructed by an in-frame G to A substitution at nt 3037.

***Capsid minus mutant.*** A VP1/VP2- mutant was generated by a 4nt deletion (3700-3703) in the capsid gene which shifted the reading frame and truncated the translation of VP1 and VP2.

**Reverse-transcriptase PCR (RT-PCR).** RT-PCR was performed with total RNA isolated from WRD cells infected with MVC GA3 virus or transfected with either the MCV infectious clone (pIMVC) or CMV NS1(spliced) cDNA. The RT-PCR was performed with Takara Blueprint RT-PCR kit (Clonetech, CA). The 5'-primer CCTGTATGGATCCAGATAAAGCCA and 3'-primer GTCTCTCTCCCCATTCGGACGGCGTG were used for the RT-PCR.

**DNA sequencing.** Sequence analysis of DNA fragments from RT-PCR experiments was done by the University of Missouri DNA Core Facility.

**Ribonuclease protection assays (RPAs).** Total and cytoplasmic RNAs were isolated using TRIzol reagent (Invitrogen), and RNase protection assays (RPAs) were performed as previously described (84). Two distinct MVC homologous RNase protection probes were used in this study. A proximal polyadenylation probe [the (pA)p probe](53) which spanned MVC nt 3107 to 3333 distinguished RNAs that were polyadenylated either proximally at (pA)p or at the distal site (pA)d, and a capsid probe (the Cap-gene probe) which spanned nt 2941 to 3333, distinguished individual RNA transcripts that were polyadenylated at either site, as well as RNAs resulting from splicing at the 3A acceptor. The location of these probes relative to the MVC genome is shown in Fig. 3A. These probes were generated from linearized templates by in vitro transcription using SP6 polymerase, as previously described (84). RNA hybridizations for RPAs were done in substantial probe excess, and RPA signals were analyzed with the Typhoon FLA9000 and quantified with MultiGuage

software (GE). Relative molar ratios of individual RNA species were calculated after adjustment for the number of $^{32}$P-labeled uridines in each protected fragment as previously described (84).

## RESULTS

### SINGLE-CYCLE INFECTIONS

We initially performed a detailed characterization of a low multiplicity, single-cycle MVC infection of para-synchronized canine WRD cells. Single-cycle kinetics were established by performing infections in the presence of neutralizing antibody, whose activity in this regard had been validated by the ability to prevent viral infection of naïve cells (data not shown). Figure 3-1 A shows the co-ordinate expression over 36 hrs of replicating viral DNA, the various major mRNAs as previously described, and the major nonstructural NS1 protein, the NP1 protein, and the capsid proteins VP1 and VP2. Viral RNA was analyzed using an RNase protection probe across the internal polyadenylation site (pA)p [probe (pA)p], Fig. 3-3. This probe distinguished RNAs that read-through (pA)p (indicated by RT in the figure) versus RNAs polyadenylated internally at (pA)p. A full transcription map generated previously (28), updated as described below, is shown in Fig. 3A. Internal polyadenylation at (pA)p actually occurs at 4 sites within a 120 nt region in that area (Fasina and Pintel, in preparation), similar to what has been seen for B19 (37). Under the para-synchronous conditions used, no differences in the ratios of the relative macromolecular forms were detected, only a continual increase in all forms.

Viral infection generated two nonstructural proteins of approximately 66 and 84 kDa in size, respectively, that reacted with an antibody to an epitope from aa 687-700 in the COOH- terminus of these proteins. This was unexpected, as the large ORF that comprises the purported NS1 gene would be predicted to

encode only the larger protein. The derivation of these two proteins will be discussed further below. Immunofluoresence assays demonstrated that NS1 proteins were primarily nuclear throughout infection, as seen for the NS1 proteins of other autonomous parvoviruses, while the NP1 protein was seen both in the nucleus and cytoplasm (Fig. 3-1B). Immunoblots assaying remaining protein after cyclohexamide inhibition indicated that both NS1 species were very stable while the NP1 protein had an intermediate stability (Fig. 3-1C). Quantification of multiple experiments showed that both NS1 proteins had a half-life of at least 10-12 hrs, while the NP1 protein had a half-life of approximately 6-8 hrs.

**Figure 3-1 Characterization of the kinetics of single-cycle MVC infection in para-synchronized permissive WRD cells.** A. Left Panel: DNA Replication**.** Southern blot analysis of samples taken from MVC infected WRD cells in the presence of a neutralizing antibody as described in the text. Representative samples were taken at 12, 18, 24 or 36 hrs following infection as shown in lanes 1, 2, 3, and 4 respectively. Viral DNA replication is evidenced by the presence of monomer and dimer replication intermediates. Identification of strand (SS) DNA is also indicated but is underrepresented in this experiment. Middle Panel: RNA Expression. Ribonuclease protection assay (RPA) showing RNA expression from the same single cycle MVC infection shown in A., left. The (pA)p probe described in Fig. 3-3A was used to detect RNA expression. The relative size of the probe is shown on the left and RNA transcripts are seen in lanes 1-4. Read-through transcripts that polyadenyate at the distal polyadenylation site (pA)d are represented as RT. Transcripts that are polyadenylated at the proximal site are indicated as (pA)p. Right Panel: Expression of NS1, NP1 and Capsid proteins. Immunoblots of cell extracts from a time course of single cycle MVC infection probed with anti-NS1, anti-NP1 or anti-capsid antibodies as described in the Materials and Methods. Cellular tubulin was used as a loading control. B. Localization of NS1 and NP1 proteins. Cellular localization of NS1 (top panel) and NP1 proteins (lower panel) using specific antibodies as described in the Materials and Methods. DAPI was used as a nuclear counterstain. C. Stability of NS1 and NP1 proteins. Immunoblots of extracts harvested at 0, 2, 4, 6, 8, and 10 hrs following cycloheximide treatment of MVC infected WRD cells. The relative

levels of the two forms of the NS1 protein, approx. 84 kDa and 66 kDa are shown in the top panel. The expression of NP is shown in the lower panel and cellular tubulin is shown as a control for the amount of protein loaded per lane.

**Figure 3-1 Characterization of the kinetics of single-cycle MVC infection in para-synchronized permissive WRD cells.**

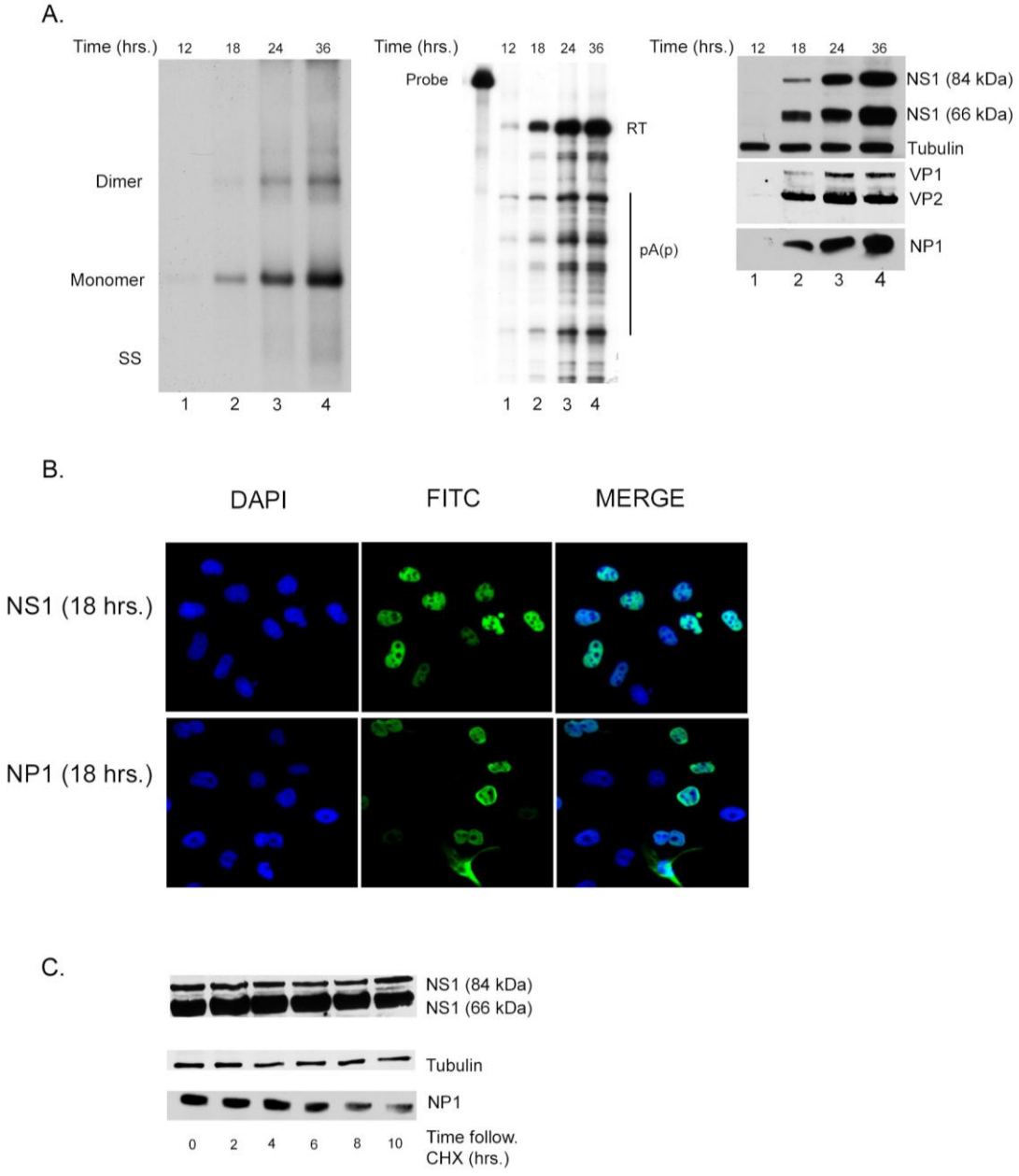

**MVC GENERATES TWO NS PROTEINS**

We were surprised to see that viral infection generated two abundant proteins that reacted with an antibody directed against the COOH-terminus of NS1. As mentioned, the NS1 gene ORF would be predicted to encode the larger protein, and the single, unspliced mRNA species identified as expressed from this gene would generate such a protein.

To begin to determine the origin of the smaller NS1 protein, we repeated our virally-infected cell immunoblots using an antibody developed against the amino-terminus of NS1. This antibody also detected both the 84 kDa and 66 kDa (Fig. 3-2A, left panel). Suspecting at first that the larger protein might be either processed or alternatively initiated to generate the smaller protein, we tagged the NS1 ORF in a CMV-driven expression vector with HA at either the amino or carboxyl termini. The smaller protein generated from both these constructs reacted with anti-HA antibody, suggesting that the smaller protein and larger proteins contained the same termini (data not shown). This led us to suspect that these constructs generated a previously undetected spliced mRNA that encoded the 66 kDa protein. RT-PCR using primers at the ends of the NS1 gene identified a spliced product in the expression constructs (data not shown), and additional RT-PCR assays showed that similar-sized spliced RNA was generated by both the wild-type infectious MVC clone (Fig. 3-2A, center panel, lane 3) and the original Cornell strain GA3 virus as well (Fig. 3-2A, center panel, lane 1). Sequencing of the cDNA product identified a splice that joined a previously unidentified donor at nt 1272 with the previously identified A1 acceptor (Fig. 3-

2B). This mRNA is expected to be approximately 3.2 kb in size, and was predicted to encode a NS protein of approximately 66 kDa. When the NS1 gene representing this cDNA was cloned into a CMV expression vector, a similar 66 kDa protein was produced (Fig. 3-2A, right panel). As expected, this clone also generated the same size spliced RNA (Fig. 3-2A, center panel, lane 5). A revised transcription map showing the additional spliced species (R1' and R2') is shown in Fig. 3-3A.

**Figure 3-2 MVC generates two NS1 proteins during viral replication.** A. Left Panel: NS1 Expression. Immunoblot of mock (M) or virus-infected (VI) WRD cell extracts probed with either an N- or C- terminus specific anti-NS1 antibody showing the expression of two distinct NS1 proteins. Middle Panel: RT-PCR. RT-PCR using 5' and 3' primers as described in the Materials and Methods was done in the presence or absence of reverse transcriptase (RT). cDNA products from the RT-PCR reaction are shown for GA3 virus infection (lane 1), WT pIMVC (lane 2), and the 1272-2199 cDNA (lane 5). Right Panel: Expression of spliced NS1/pcDNA. Immunoblot of 293T cell extracts transfected with either WT pIMVC or NS1 1272-2199/cDNA probed with an anti-NS1 (C-terminus specific) antibody. B. NS1 DNA sequence analysis. Alignment of the nucleotide sequence of MVC and NS1 1272-2199/cDNA are shown. The regions depicted are from nt 1220-1272 and nt 2168-2260. The dashed lines in the NS1 1272-2199/cDNA sequence represent the spliced region from the newly identified 1D'-1A intron.

**Figure 3-2 MVC generates two NS1 proteins during viral replication.**

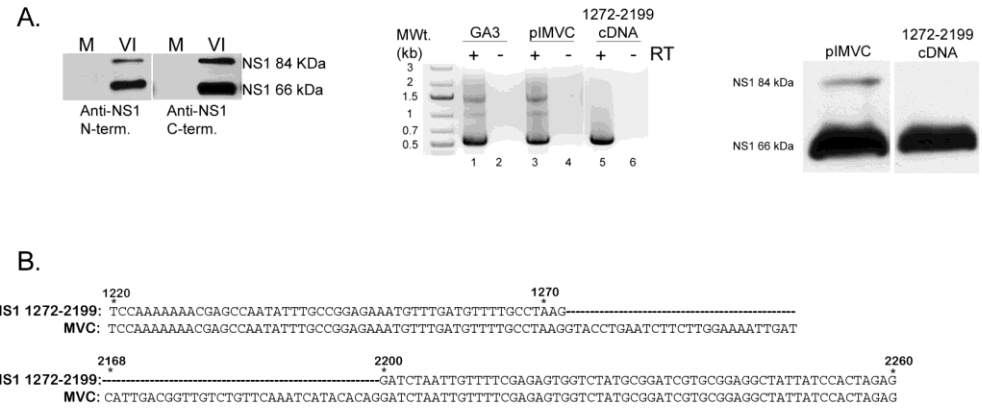

## NP1 MUTANTS HAVE A SIGNIFICANT EFFECT ON RNA PROCESSING INDEPENDENT OF GENOME REPLICATION

As previously reported, termination mutations that prevented production of either the NS1 proteins or NP1 greatly inhibited replication of the MVC infectious clone (28). In addition to its anticipated role in viral genome replication, we could detect no evidence that NS1 played a role in transactivation of the viral P6 promoter or in RNA processing (data not shown). In contrast however, we observed that NP1 mutants displayed a striking phenotype in which the profile of accumulated RNA forms were altered, in a manner that was mainly independent of replication. As mentioned, NP1 is unique to the bocaviruses. It currently has no apparent homologue in the data base.

As can be seen by the RNase protection assays using a probe that spanned the (pA)p site, following either viral infection (Fig. 3-1, middle panel) or transfection of the replicating infectious clone (Fig. 3-4A, lane 2), the majority of wild-type MVC RNAs read through the internal polyadenylation site (pA)p, extend through the capsid gene, and polyadenylate at the (pA)d site at the right hand end. However, three individual mutants of the infectious clone containing premature translation termination mutations within the NP1 coding region all show a very different phenotype: the majority of the steady state RNA in total RNA preparations generated from these mutants do not extend beyond the internal polyadenylation site (Fig. 3-4A, NP1-2735TAG, NP1-2740TAA, and NP1-2839TAA, lanes 3-5; see mutant diagram in Fig. 3-3B).

It has been suggested that the processing of B19 RNA is governed by replication of the viral genome (85). Although NP1 mutants are deficient for viral replication, the RNA phenotype we observed is not governed by genome replication: a non-replicating MVC “rep/cap” like construct lacking the viral hairpins (RC WT), a non-replicating hairpin-containing NS1 mutant of the MVC infectious clone (pIMVC-NS1-), and a mutant severely impaired for replication due to deletion mutations in the right-hand end hairpin acquired during passage of the infectious clone in recombination-proficient E. *coli* (pIMVC-FD), all displayed an RNA phenotype indistinguishable from viral infection (Fig. 3-4B, RC WT, pIMVC-NS1(-), pIMVC-FD, compare lanes 3, 5, and 6 to wild-type, lane 2 and NP1-2735TAG, lane 4). Results with pIMVC-NS1(-) also indicated that the phenotype that was observed was independent of NS1.

To rule out non-specific *cis*-acting effects of the introduction of termination mutations in the NP1 coding region we also generated and characterized a single nt mutation destroying the NP1 AUG (NP1-ATGm), and another that introduced a series of 5 proline mutations in the center of the NP1 coding region (NP1-5XPro) in the non-replicating rep/cap construct. These mutations had the same phenotype as the termination mutations (Fig. 3-4C, NP1-ATGm, NP1-5XPro, compare lanes 4 and 5 to lane 6).

The termination mutations so far described in NP1 exist within the third intron. It was therefore possible that the primary effect of these mutations was on splicing of this intron, which subsequently affected downstream polyadenylation. This was unlikely for the following reasons. First, an acceptor

mutation in the MVC rep/cap background that prevented splicing of the third intron had no effect on the relative use of the two polyadenylation sites (Fig. 3-4C, 3Am, compare lane 3 to 2). An RPA utilizing the Cap-gene probe (diagrammed in Fig. 3-3A) that monitors splicing of the third intron confirmed that this mutant did not generate RNAs spliced at this acceptor (Fig. 3-4D, compare lane 5 to lanes 3 or 4). Secondly, a single nucleotide mutation in the rep/cap background downstream of the third intron, designed to inactivate NP1 by fusing it to the capsid ORF had the same phenotype as seen for the other NP1 mutations (data not shown).

**Figure 3- 3 Revised genetic map of MVC**. A. The genetic map of MVC drawn to scale highlighting the P6 promoter, splice donors (D) and acceptors (A), and the proximal (pA)p and distal (pA)d polyadenylation sites. The numbers denote the nucleotide positions within the MVC genome. The newly identified splice site (1D' – 1A) as used in RNAs R1' and R2' is incorporated in the map. The location of the Cap-gene and (pA)p probes relative to the MVC genome is shown. B. A diagram (not to scale) indicating the relative locations of the NP1 termination mutants NP1-2735TAG, NP1-2740TAA, and NP1-2839TAA, and the NP1- 5XPro mutant.

**Figure 3-3 Revised genetic map of MVC.**

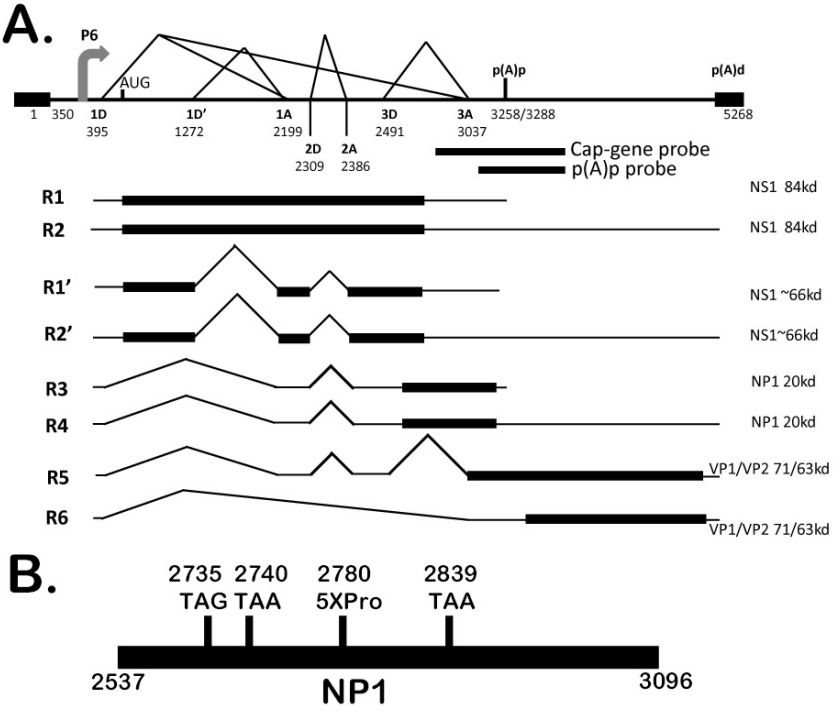

Figure 3-4E shows a quantification of multiple experiments with these mutants, both in a replication deficient “rep/cap” background (TR-), and within the replicating infectious clone (TR+). The NP1-5XPro and NP1-2735TAG constructs showed a greater than 10-fold increase in relative internal polyadenylation, while the 3Am mutant performed like wild-type. It is not yet clear why there is a difference (albeit statistically insignificant) in the polyadenylation ratios of the NP1-2735TAG construct in replicating versus nonreplicating backgrounds.

The previous analysis monitored levels of RNA that were alternatively polyadenylated at either (pA)p or (pA)d. To determine which MVC RNAs had been specifically affected by the lack of NP1 function we utilized an RNase protection assay using the Cap-gene probe that specifically distinguished relative levels of i) R1+R3, which utilized (pA)p and encode NS1 and NP1, respectively; ii) read-through R2 + R4, which encode NS1 and NP1, respectively; and iii) the read-through R5 + R6 mRNAs, which together encode capsid proteins. As described above, the wild-type virus and infectious clone encode primarily read-through products, and these can here be seen to include both the R2 and R4 mRNAs, as well as predominantly the capsid-encoding R5 and R6 mRNAs (Fig. 3-4F, lanes 2, 3). RNase protections of RNA generated from the NP1 mutants using this probe showed a deficiency in the accumulation of both the read-through R2 + R4 mRNA, and a drastic reduction in the capsid encoding mRNAs R5 and R6 (Fig.3- 4F, lanes 4-6). Both the NP1-2735TAG mutant and the NP1-5XPro mutant generated dramatically reduced levels of VP1 and VP2, although

they both expressed NS1, and the NP1-5XPro mutant generated high levels of NP1 (Fig. 3-4 G, lanes 3 and 4).

Taken together, our results demonstrate that NP1 has a significant effect on viral RNA processing, and that in the absence of wild-type NP1, read-through of the internal (pA)p site, which is necessary to access the capsid gene ORF, is deficient.

**Figure 3-4 MVC NP1 mutants have a significant effect on RNA processing independent of genome replication.** A. RNA expression determined by RNase protection assay (RPA). WRD cells were transfected with the wild-type infectious clone pIMVC (lane 2) or three distinct NP1 termination mutants, NP1-2735TAG, NP1-2740TAA or NP1-2839TAA, (lanes 3, 4, and 5). At 2 days post-transfection, total RNAs were isolated and probed for MVC-specific mRNAs using the (pA)p probe that is depicted in Fig. 3A. The sizes of protected bands are shown on the left and the designated (pA)d or (pA)p RNA species are shown on the right. The RNA probe is shown in lane 1. B. RNAse protection assays using the (pA)p probe showing RNA expression of WRD cells transfected with WT pIMVC (lane 2) or replication-deficient mutants: RC WT, NP1-2735TAG, pIMVC-NS1-, and pIMVC-FD, as described in the text (lanes 3, 4, 5 and 6, respectively). The (pA)p probe is shown in lane 1. RNA species are designated as (pA)d or (pA)p. C. RNA expression assayed by RPAs using the (pA)p probe of WRD cells transfected with WT pIMVC (lane 2), or 3A mutant (lane 3) or NP1- mutants, ATGm (lane 4), 5XPro (lane 5) or NP1-2735TAG (lane 6) as described in the text. The (pA)p probe is shown in lane 1. RNA species are designated as (pA)d or (pA)p. D. RPA utilizing the Cap-gene probe as depicted in Fig. 3A of either virus infected WRD cells (VI, lane 3), or WRD cells transfected with WT pIMVC (lane 4), or the third intron splice mutant 3Am (lane 5) as described in the text. The WT Cap-gene probe (lane 1) and the homologous 3A Cap-gene probe (lane 2) are shown. Individual RNA species and their relative sizes are designated on the right and left of the image. E. Quantification of RPAs showing the average polyadenylation

ratios [(pA)p/(pA)d] of RNA transcripts from WT pIMVC, 3Am, NP1-5XPro, or NP1-2735TAG in either a replicating infectious clone (TR+) or replicating-deficient (TR-) background. Error bars indicate the standard deviation from 3 independent experiments. F. RPA utilizing the Cap-gene probe (lane 1) showing RNA expression distinguishing individual transcripts from viral infection (lane 2), transfection of WT pIMVC (lane 3), or transfection of NP1 mutants 2735TAG, 2740TAA, and 2839TAA (lanes 4, 5, and 6). Individual RNA species R1-R6 are labeled on the right and their respective sizes shown on the left. G. Expression of NP1, NS1 and capsid proteins. Immunoblots of 293T cell extracts either mock transfected or transfected with WT pIMVC, NP1 termination mutant NP1-2735TAG, or NP1 proline mutant NP1-5XPro, probed with anti-NS1, anti-NP1 or anti-capsid antibodies

**Figure 3-4 MVC NP1 mutants have a significant effect on RNA processing independent of genome replication, Panels A and B.**

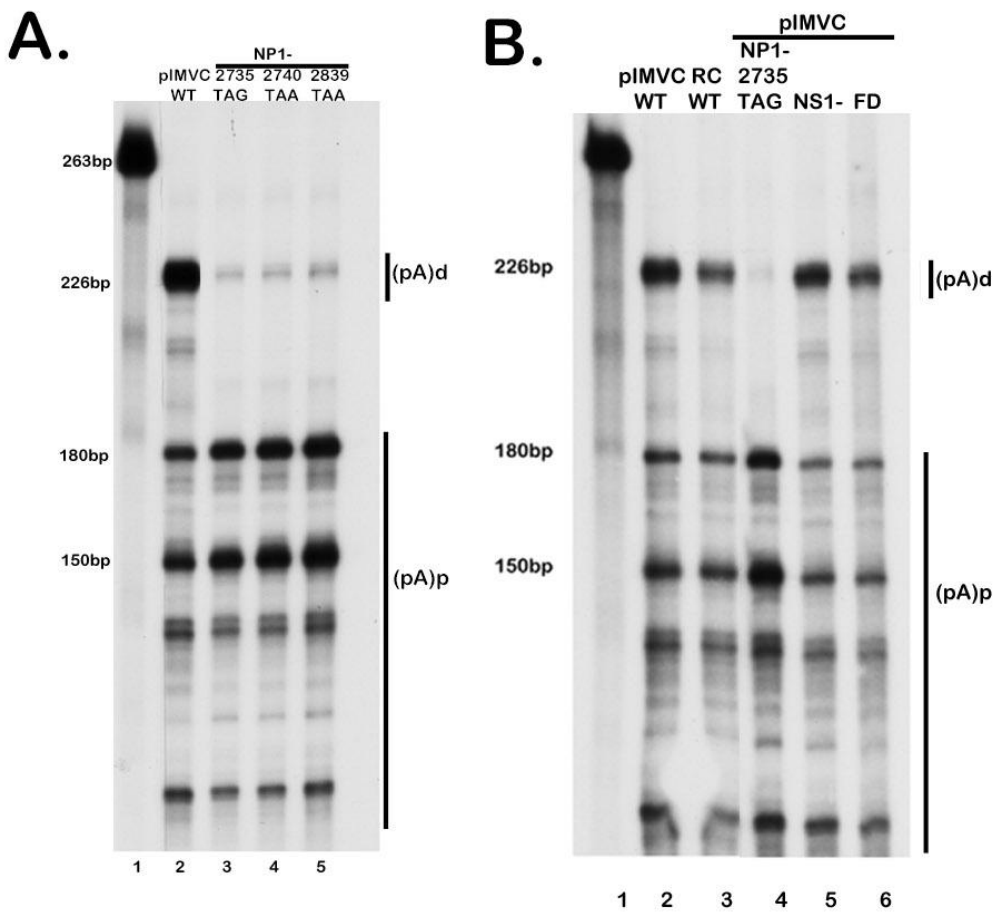

**Figure 3-4 MVC NP1 mutants have a significant effect on RNA processing independent of genome replication, Panels C and D.**

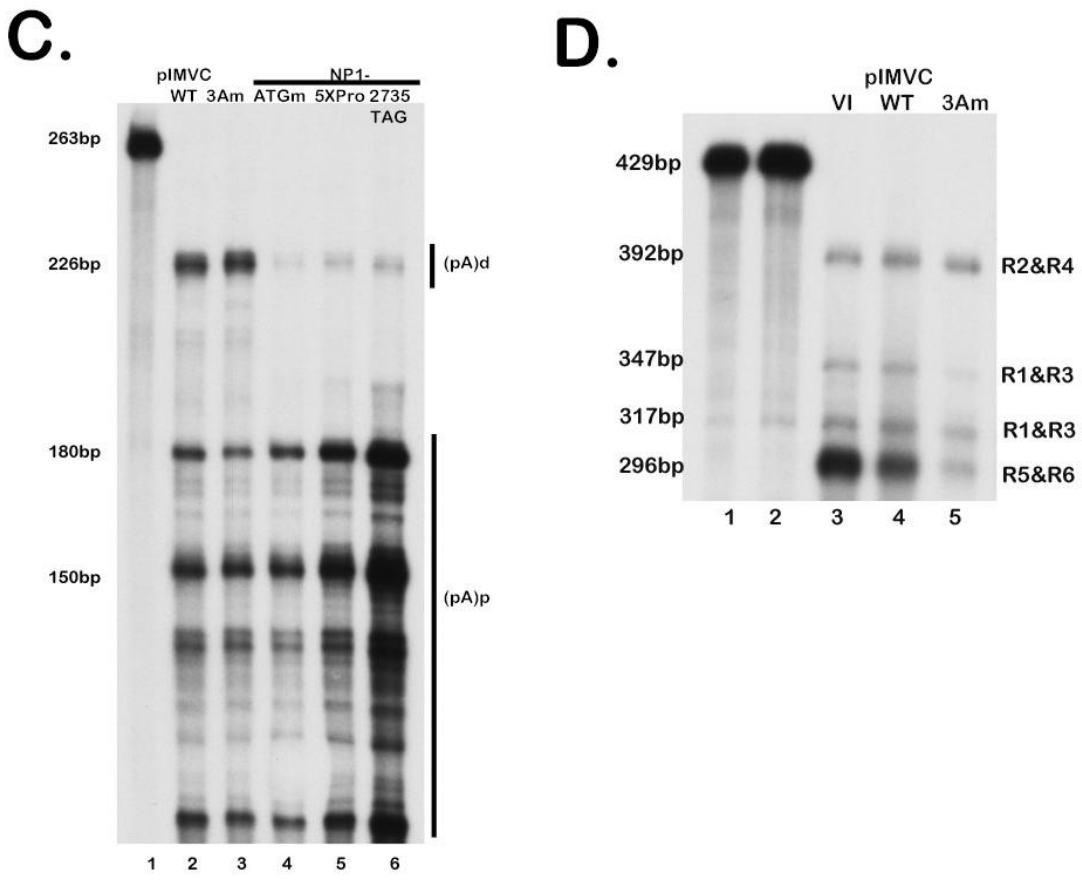

**Figure 3-4 MVC NP1 mutants have a significant effect on RNA processing independent of genome replication, Panels E, F and G.**

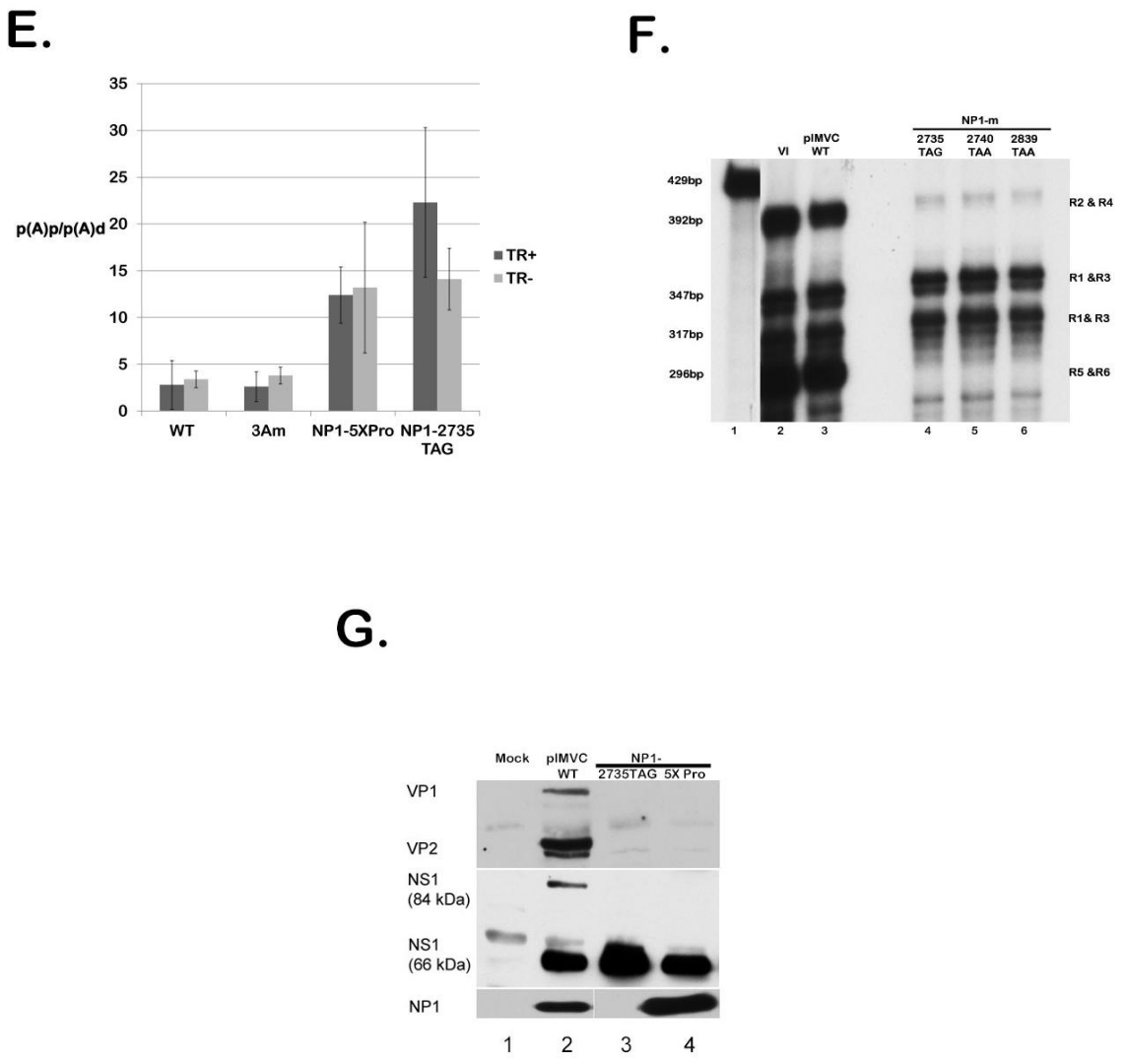

If the sole defect of the NP1 mutants were a deficiency in capsid protein production, NP1 mutants in a replicating background should replicate similarly to a capsid (-) mutant, i.e., they should generate the double-stranded 5kb monomer RF forms, yet no ssDNA. However, in multiple experiments (in which re-infection was blocked), the NP1 mutants were found to be more deficient in generating the mRF replicative forms than a capsid-minus mutant [Fig. 3-5A, compare lanes 3 (NP1-2735TAG) and 4 (NP1-5XPro), to lane 5 (Cap minus)]; and to viral infection, lane 1 and pIMVC, lane 2]. This suggested that NP1 has at least one additional function during viral replication.

**Figure 3-5 NP1 mutants exhibit a greater defect in viral replication than a capsid minus mutant.** Southern blot analysis of samples taken from WRD cells infected with MVC (lane 1), or transfected with the following: WT pIMVC (lane 2), NP1 mutant (NP1-2735TAG) (lane 3), NP1-5XPro (lane 4), or a capsid minus mutant described in Materials and Methods (lane 5). The infection or transfections were done in the presence of a neutralizing antibody and southern blot analyses were done as described in the text. Total DNA content was measured and equivalent amounts of total DNA were loaded in each lane. DNA replication forms are indicated by monomer, dimer and single strand (SS) DNA.

**Figure 3-5 NP1 mutants exhibit a greater defect in viral replication than a capsid minus mutant.**

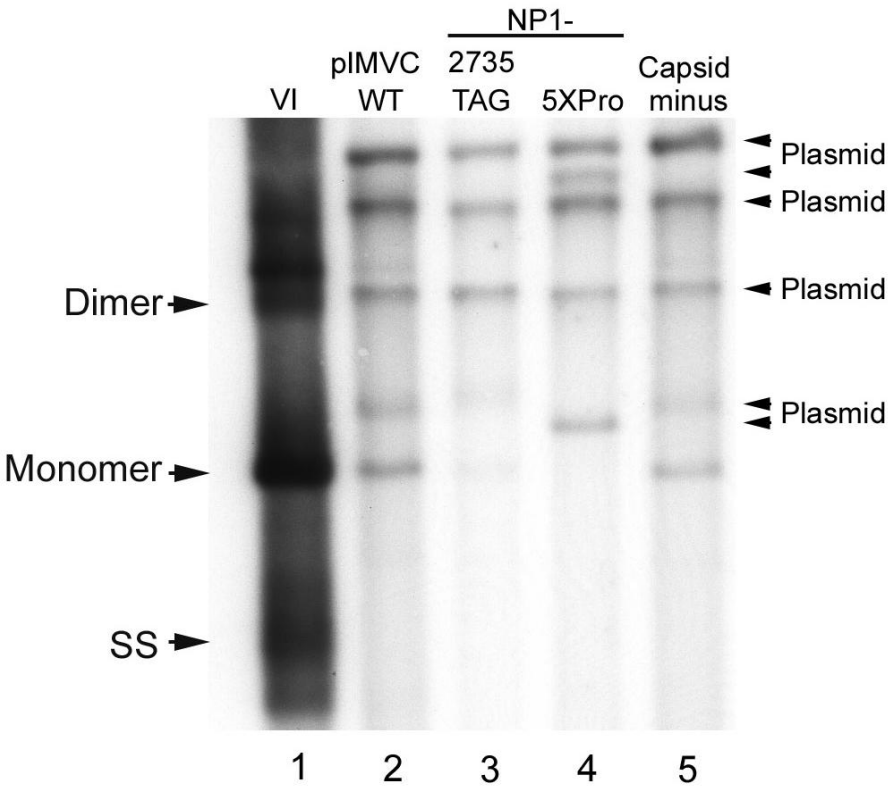

## DISCUSSION

In this chapter we first present a characterization of a single cycle bocavirus infection. In the course of this analysis we have identified a second nonstructural protein, and determined its origin from a previously unidentified spliced mRNA. The second protein lacks the typical Walker-type helicase motifs(86), and so may fall into the category of parvovirus nonstructural proteins lacking helicase activity, like MVM NS2(87).

Perhaps most importantly, we have also shown that the MVC NP1 protein is required for read-through of the internal polyadenylation site, and access into the capsid gene. This is the first parvovirus protein shown to have a direct effect on RNA processing.

It is not known how NP1 functions. It could be directly at the level of splicing, poyadenylation, or export. Its activity is independent of genome replication, independent of NS1 function, and not due to effects on splicing of the upstream 3D/3A intron. Attempts at complementing the NP1mutants with NP1 in *trans* have as yet been only partially successful; however, multiple types of mutations, at different places within NP1, including missense, nonsense, frame-shift, and initiating AUG mutations all have similar phenotypes. Interestingly, it has been pointed out to us (Florence Baudin, personal communication) that NP1 has multiple arginine/serine di-repeats characteristic of an SR protein, a class known to function in RNA processing(88).

Although parvoviruses have only subtle early to late expression shifts, they all mediate access to their capsid genes, and different parvoviruses do so in different ways. Those parvoviruses with separate capsid gene promoters, like the *Parvovirus* MVM (89) and the *Dependovirus* AAV (6, 53, 90), do so by transcriptional trans-activation of those promoters. The *Erythroviruses* (91) have a single promoter at the left-hand end of the genome and a polyadenylation site within an intron in the center of the genome. Splicing of this intron to remove the polyadenylation signal helps govern access to the capsid gene for these viruses (92). The *Amdoviruses* (93-94) and the *Bocaviruses* (77) have polyadenylation sites that lie within their capsid gene; however, these potent motifs are retained in the capsid-encoding mRNA and must be somehow suppressed to allow export and accumulation of mRNAs that encode capsid protein information. We have shown here that the bocavirus MVC has evolved yet another way to allow essential access to its capsid protein gene, namely, by the action of its novel NP1 protein, which is required to read-through its internal (pA)p site.

# CHAPTER IV

# SUMMARY

## THESIS SUMMARY

The research presented in this thesis focuses on post-translational modifications and the functional roles of parvovirus non-structural proteins. Work presented in Chapter 2 summarizes findings on the ubiquitination and degradation of AAV large Rep proteins in the context of the adenovirus E3 ubiquitin ligase. In Chapter 3 studies on the bocavirus MVC virus led to the discovery of a new non-structural protein and more importantly, identified a function for this novel NP1 protein.

Previous work done in our lab has shown that full replication of AAV5 requires all five Ad helper components. However, although E4orf6 was required for genomic replication together with E1b 55K these proteins selectively targeted AAV small Rep and Cap proteins for proteasomal degradation via the participation of the Ad E3 ubiquitin ligase (11, 48). Additionally, in collaboration with a former graduate student, we also showed that AAV small Rep proteins are modified by different forms of ubiquitination (48).

Results described in Chapter 2 demonstrated for the first time that AAV2 large Rep proteins (Rep 78/68) are modified by ubiquitination following viral infection with Ad5. Furthermore, large Rep proteins are degraded in the presence of E4orf6 in E1b 55k containing 293T cells. This degradation can be reversed by addition of the proteasome inhibitor MG132. The loss of Rep in the presence of Ad E4orf6 and E1b 55k suggested that the Ad E3 ubiquitin ligase may participate in this degradation. To further study the degradation of large Rep an in vitro

ubiquitination assay was developed. This assay showed that AAV types 2 and 5 large Rep proteins are ubiquitinated following co-transfection with a plasmid expressing ubiquitin. Furthermore, it was also shown that the large Rep proteins are polyubiquitinated both in the presence and absence of E4orf6 /E1b 55k, implying that large Rep may be modified by different forms of ubiquitination. Surprisingly, and in contrast to results with AAV Rep 52, the large Rep proteins of AAV2 exhibited lysine 48-linked ubiquitination in both the presence and absence of E4orf6. These results suggested that the targeting of large Rep for the lysine 48 (K48) form of ubiquitination can be accomplished by a ligase(s) other than the Ad E3 ubiquitin ligase. It has recently been shown that a cellular ubiquitin ligase EDD1 forms a complex with AAV2 large Rep proteins, thus this ligase may be a candidate for this reaction (51). Similar to results with small Rep52, Rep 78/68 is also ubiquitinated via a lysine 63 (K63) linkage in either the presence or absence of E4orf6/E1b 55k suggesting that large Rep may have functions in signaling, trafficking or DNA damage responses.

The E4orf6/E1b 55k mediated ubiquitination and proteasomal degradation of large Rep is reversed by addition of a dominant negative ubiqutin. Large Rep proteins can be found in complexes with E1b 55k and cullin 5, and levels of Rep K48 ubiquitination are decreased following siRNA knockdown of cullin 5. Collectively, these data implicate the involvement of the Ad E3 ubiqutin ligase in the proteasomal degradation of AAV large rep. Although its role in infection is not yet understood, the ubiquitination and accelerated proteasomal degradation of

AAV large Rep proteins, particularly in the presence of Ad E4orf6 and E1b 55k may represent important regulatory events in the AAV life cycle.

The research summarized in Chapter 3 led to two important findings. First a detailed characterization of a single cycle MVC infection was performed in permissive canine cells. In these experiments viral DNA replication, RNA expression, protein expression, protein stability, and cellular localization of MVC non-structural proteins were examined. During the course of these studies a new nonstructural protein (NS) within the MVC genome was identified. Using biochemical and genetic approaches it was determined that this new NS protein is derived from a doubly spliced mRNA within the larger NS gene. This has led to a revision of the previously published transcription map. Sequence analysis revealed that the newly identified smaller NS protein in MVC lacks the characteristic Walker-type helicase motifs making it similar to the previously described MVM small non-structural protein NS2. The role this newly identified protein plays in viral replication is currently being investigated.

NP1 expression is unique to the members of the bocavirus genus. An important goal in the study reported in Chapter 3 is to better understand the role this protein plays in the MVC viral life cycle. Data presented in this chapter shows that the NP1 protein is required for read-through of the internal polyadenylation site, and access to the capsid gene. Interestingly, NP1 is the first parvovirus protein implicated to have a direct effect on viral RNA processing.

Using multiple approaches we demonstrated that mutants of NP1 showed a dramatic shift in transcripts that are polyadenylated proximally relative to those polyadenylated at the distal site. This phenotype was observed with a number of mutants containing targeted mutations at different sites within the NP1 gene, including missense, nonsense, frame-shift, and initiating AUG mutations. NP1 activity is independent of genome replication, independent of NS1 function, and independent of splicing of the 3D/3A intron. Experiments aimed at complementing NP1mutants with NP1 in trans are on-going.

It is not known how NP1 functions to allow read through of the internal polyadenylation signal. Preliminary structure prediction analysis has shown that NP1 has a highly disordered N-terminus region (data not shown). Recent, more in depth analyses revealed that this disordered region has an abundance of arginine/serine (RS) motifs, indicative of an SR protein. SR proteins are a class of RNA-binding proteins that can affect all aspects of RNA metabolism including, pre-mRNA splicing, polyadenylation, RNA export, RNA stability, and translation (88). We predict that NP1 is an RNA binding protein and future work will investigate this hypothesis in an effort to decipher the mechanism of NP1 action.

The accumulation of appropriate levels of capsid protein is considered to be a rate-limiting step in order for parvoviruses to achieve productive infections. Interestingly, these viruses attain the proper levels of capsid expression by a number of different strategies. Parvoviruses with multiple promoters such as MVM or AAV2 encode a capsid-specific promoter to generate capsid transcripts. Furthermore, these viruses also regulate capsid transcription by transactivating

the capsid promoter via the actions of their large non-structural proteins. Unlike MVM or AAV, parvoviruses that encode a single promoter like the B19 virus must permit read through of their internal polyadenylation signal by a mechanism that does not rely on promoter transactivation. The internal polyadenylation site of B19 is within an intron in the center of the genome. As such, splicing of this intron to remove the polyadenylation signal helps facilitate access to the capsid gene. It has also been shown that for the B19 virus genome replication results in an increase in transcripts that are polyadenylated at the distal site. Unlike B19, both Aleutian mink disease virus (AMDV) and MVC have polyadenylation sites that reside within the coding region of the capsid gene. Consequently, splicing within this region is not a viable option to allow access to capsid transcripts. We have shown in Chapter 3 that MVC utilizes an innovative way to gain access to its capsid gene, it does so by the action of its novel NP1 protein which is required to read-through its internal (pA)p site.

In summary, parvoviruses due to their compact genomes rely on a diverse set of transcriptional and post-transcriptional strategies to generate the proteins required for replication and virion production. MVC a parvovirus encoding a single promoter uses its unique gene product NP1 to regulate an important post-transcriptional process, alternative polyadenylation, in order to achieve productive infection.

# REFERENCES
## References


1. Berns, K.I., *Parvovirus replication.* Microbiol Rev, 1990. 54(3): p. 316-29.
2. Tattersall, P., ed. *The evolution of Parvovirus taxonomy, p 5-14*. Parvoviruses, ed. S.F.C. J.Kerr, M. E. Bloom, R. M. Linden, and C. R. Parrish 2006, Hodder Arnold, United Kingdom.
3. Atchison, R.W., B.C. Casto, and W.M. Hammon, *Adenovirus-Associated Defective Virus Particles.* Science, 1965. 149(3685): p. 754-6.
4. Weitzman, M.D. and R.M. Linden, *Adeno-associated virus biology.* Methods Mol Biol. 807: p. 1-23.
5. Dutheil, N., et al., *Adeno-associated virus site-specifically integrates into a muscle-specific DNA region.* Proc Natl Acad Sci U S A, 2000. 97(9): p. 4862-6.
6. Qiu, J. and D. Pintel, *Processing of adeno-associated virus RNA.* Front Biosci, 2008. 13: p. 3101-15.
7. Sonntag, F., K. Schmidt, and J.A. Kleinschmidt, *A viral assembly factor promotes AAV2 capsid formation in the nucleolus.* Proc Natl Acad Sci U S A. 107(22): p. 10220-5.
8. Farris, K.D. and D.J. Pintel, *Adeno-associated virus type 5 utilizes alternative translation initiation to encode a small Rep40-like protein.* J Virol. 84(2): p. 1193-7.
9. Ferrari, F.K., et al., *Second-strand synthesis is a rate-limiting step for efficient transduction by recombinant adeno-associated virus vectors.* J Virol, 1996. 70(5): p. 3227-34.
10. Nayak, R. and D.J. Pintel, *Positive and negative effects of adenovirus type 5 helper functions on adeno-associated virus type 5 (AAV5) protein accumulation govern AAV5 virus production.* J Virol, 2007. 81(5): p. 2205-12.
11. Nayak, R., K.D. Farris, and D.J. Pintel, *E4Orf6-E1B-55k-dependent degradation of de novo-generated adeno-associated virus type 5 Rep52 and capsid proteins employs a cullin 5-containing E3 ligase complex.* J Virol, 2008. 82(7): p. 3803-8.
12. Farris, K.D., et al., *Adeno-associated virus small rep proteins are modified with at least two types of polyubiquitination.* J Virol. 84(2): p. 1206-11.
13. Thimmappaya, B., et al., *Adenovirus VAI RNA is required for efficient translation of viral mRNAs at late times after infection.* Cell, 1982. 31(3 Pt 2): p. 543-51.

14. Nayak, R. and D.J. Pintel, *Adeno-associated viruses can induce phosphorylation of eIF2alpha via PKR activation, which can be overcome by helper adenovirus type 5 virus-associated RNA.* J Virol, 2007. 81(21): p. 11908-16.
15. Duan, D., et al., *Circular intermediates of recombinant adeno-associated virus have defined structural characteristics responsible for long-term episomal persistence in muscle tissue.* J Virol, 1998. 72(11): p. 8568-77.
16. Qing, K., et al., *Role of tyrosine phosphorylation of a cellular protein in adeno-associated virus 2-mediated transgene expression.* Proc Natl Acad Sci U S A, 1997. 94(20): p. 10879-84.
17. Blackford, A.N. and R.J. Grand, *Adenovirus E1B 55-kilodalton protein: multiple roles in viral infection and cell transformation.* J Virol, 2009. 83(9): p. 4000-12.
18. Ciechanover, A., *The ubiquitin-mediated proteolytic pathway.* Brain Pathol, 1993. 3(1): p. 67-75.
19. Blanchette, P. and P.E. Branton, *Manipulation of the ubiquitin-proteasome pathway by small DNA tumor viruses.* Virology, 2009. 384(2): p. 317-23.
20. Komander, D., *The emerging complexity of protein ubiquitination.* Biochem Soc Trans, 2009. 37(Pt 5): p. 937-53.
21. Haglund, K. and I. Dikic, *Ubiquitylation and cell signaling.* Embo J, 2005. 24(19): p. 3353-9.
22. Finley, D., *Recognition and processing of ubiquitin-protein conjugates by the proteasome.* Annu Rev Biochem, 2009. 78: p. 477-513.
23. Jin, L., et al., *Mechanism of ubiquitin-chain formation by the human anaphase-promoting complex.* Cell, 2008. 133(4): p. 653-65.
24. Kapoor, A., et al., *A newly identified bocavirus species in human stool.* J Infect Dis, 2009. 199(2): p. 196-200.
25. Allander, T., et al., *Human bocavirus and acute wheezing in children.* Clin Infect Dis, 2007. 44(7): p. 904-10.
26. Huang, Q., et al., *Establishment of a reverse genetics system for studying human bocavirus in human airway epithelia.* PLoS Pathog. 8(8): p. e1002899.
27. Carmichael, L.E., D.H. Schlafer, and A. Hashimoto, *Minute virus of canines (MVC, canine parvovirus type-1): pathogenicity for pups and seroprevalence estimate.* J Vet Diagn Invest, 1994. 6(2): p. 165-74.
28. Sun, Y., et al., *Molecular characterization of infectious clones of the minute virus of canines reveals unique features of bocaviruses.* J Virol, 2009. 83(8): p. 3956-67.
29. Chen, A.Y., et al., *Bocavirus infection induces mitochondrion-mediated apoptosis and cell cycle arrest at G2/M phase.* J Virol. 84(11): p. 5615-26.

30. **Luo, Y., A.Y. Chen, and J. Qiu, *Bocavirus infection induces a DNA damage response that facilitates viral DNA replication and mediates cell death.* J Virol. 85(1): p. 133-45.**
31. **Miller, C.L. and D.J. Pintel, *Interaction between parvovirus NS2 protein and nuclear export factor Crm1 is important for viral egress from the nucleus of murine cells.* J Virol, 2002. 76(7): p. 3257-66.**
32. **Best, S.M., et al., *Caspase cleavage of the nonstructural protein NS1 mediates replication of Aleutian mink disease parvovirus.* J Virol, 2003. 77(9): p. 5305-12.**
33. **Schoborg, R.V. and D.J. Pintel, *Accumulation of MVM gene products is differentially regulated by transcription initiation, RNA processing and protein stability.* Virology, 1991. 181(1): p. 22-34.**
34. **Legendre, D. and J. Rommelaere, *Targeting of promoters for trans activation by a carboxy-terminal domain of the NS-1 protein of the parvovirus minute virus of mice.* J Virol, 1994. 68(12): p. 7974-85.**
35. **Pereira, D.J., D.M. McCarty, and N. Muzyczka, *The adeno-associated virus (AAV) Rep protein acts as both a repressor and an activator to regulate AAV transcription during a productive infection.* J Virol, 1997. 71(2): p. 1079-88.**
36. **Ragni, M.V., K.E. Sherman, and J.A. Jordan, *Viral pathogens.* Haemophilia. 16 Suppl 5: p. 40-6.**
37. **Yoto, Y., J. Qiu, and D.J. Pintel, *Identification and characterization of two internal cleavage and polyadenylation sites of parvovirus B19 RNA.* J Virol, 2006. 80(3): p. 1604-9.**
38. **Guan, W., et al., *Internal polyadenylation of the parvovirus B19 precursor mRNA is regulated by alternative splicing.* J Biol Chem. 286(28): p. 24793-805.**
39. **Huang, Q., et al., *Internal polyadenylation of parvoviral precursor mRNA limits progeny virus production.* Virology, 2012. 426(2): p. 167-77.**
40. **Qiu, J., F. Cheng, and D. Pintel, *The abundant R2 mRNA generated by aleutian mink disease parvovirus is tricistronic, encoding NS2, VP1, and VP2.* J Virol, 2007. 81(13): p. 6993-7000.**
41. **Cheng, F., et al., *The capsid proteins of Aleutian mink disease virus activate caspases and are specifically cleaved during infection.* J Virol. 84(6): p. 2687-96.**
42. **Berns, K.I. and C. Giraud, *Biology of adeno-associated virus.* Curr Top Microbiol Immunol, 1996. 218: p. 1-23.**
43. **Bowles, D., J. E. Rabinowitz, and R. J. Samulski, *The genus Dependoviruses*. Parvoviruses, ed. J.K.e. al. 2006, London, United Kingdom: Hodder Arnold. 15-24.**
44. **Weitzman, M.D., *The Parvovirus life cycle: an introduction to molecular interactions important for infection*. Parvoviruses, ed. J.K.e. al. 2006, London, United Kingdom. 143-156.**

45. **Blanchette, P., et al., *Both BC-box motifs of adenovirus protein E4orf6 are required to efficiently assemble an E3 ligase complex that degrades p53.* Mol Cell Biol, 2004. 24(21): p. 9619-29.**
46. **Harada, J.N., et al., *Analysis of the adenovirus E1B-55K-anchored proteome reveals its link to ubiquitination machinery.* J Virol, 2002. 76(18): p. 9194-206.**
47. **Woo, J.L. and A.J. Berk, *Adenovirus ubiquitin-protein ligase stimulates viral late mRNA nuclear export.* J Virol, 2007. 81(2): p. 575-87.**
48. **Farris, K.D., et al., *Adeno-associated virus small rep proteins are modified with at least two types of polyubiquitination.* J Virol, 2010. 84(2): p. 1206-11.**
49. **Im, D.S. and N. Muzyczka, *The AAV origin binding protein Rep68 is an ATP-dependent site-specific endonuclease with DNA helicase activity.* Cell, 1990. 61(3): p. 447-57.**
50. **Kotin, R.M., et al., *Site-specific integration by adeno-associated virus.* Proc Natl Acad Sci U S A, 1990. 87(6): p. 2211-5.**
51. **Nash, K., et al., *Identification of cellular proteins that interact with the adeno-associated virus rep protein.* J Virol, 2009. 83(1): p. 454-69.**
52. **Needham, P.G., et al., *Adeno-associated virus rep protein-mediated inhibition of transcription of the adenovirus major late promoter in vitro.* J Virol, 2006. 80(13): p. 6207-17.**
53. **Qiu, J. and D.J. Pintel, *The adeno-associated virus type 2 Rep protein regulates RNA processing via interaction with the transcription template.* Mol Cell Biol, 2002. 22(11): p. 3639-52.**
54. **Samulski, R.J., et al., *Targeted integration of adeno-associated virus (AAV) into human chromosome 19.* Embo J, 1991. 10(12): p. 3941-50.**
55. **Snyder, R.O., D.S. Im, and N. Muzyczka, *Evidence for covalent attachment of the adeno-associated virus (AAV) rep protein to the ends of the AAV genome.* J Virol, 1990. 64(12): p. 6204-13.**
56. **Zhou, X., et al., *Biochemical characterization of adeno-associated virus rep68 DNA helicase and ATPase activities.* J Virol, 1999. 73(2): p. 1580-90.**
57. **Bantel-Schaal, U., *Adeno-associated parvoviruses inhibit growth of cells derived from malignant human tumors.* Int J Cancer, 1990. 45(1): p. 190-4.**
58. **Bantel-Schaal, U., *Infection with adeno-associated parvovirus leads to increased sensitivity of mammalian cells to stress.* Virology, 1991. 182(1): p. 260-8.**
59. **Bantel-Schaal, U. and M. Stohr, *Influence of adeno-associated virus on adherence and growth properties of normal cells.* J Virol, 1992. 66(2): p. 773-9.**
60. **Timpe, J.M., K.C. Verrill, and J.P. Trempe, *Effects of adeno-associated virus on adenovirus replication and gene expression during coinfection.* J Virol, 2006. 80(16): p. 7807-15.**

61. Hunter, L.A. and R.J. Samulski, *Colocalization of adeno-associated virus Rep and capsid proteins in the nuclei of infected cells.* J Virol, 1992. 66(1): p. 317-24.
62. Baker, A., et al., *Adenovirus E4 34k and E1b 55k oncoproteins target host DNA ligase IV for proteasomal degradation.* J Virol, 2007. 81(13): p. 7034-40.
63. Cathomen, T. and M.D. Weitzman, *A functional complex of adenovirus proteins E1B-55kDa and E4orf6 is necessary to modulate the expression level of p53 but not its transcriptional activity.* J Virol, 2000. 74(23): p. 11407-12.
64. Dallaire, F., et al., *Identification of integrin alpha3 as a new substrate of the adenovirus E4orf6/E1B 55-kilodalton E3 ubiquitin ligase complex.* J Virol, 2009. 83(11): p. 5329-38.
65. Moore, M., N. Horikoshi, and T. Shenk, *Oncogenic potential of the adenovirus E4orf6 protein.* Proc Natl Acad Sci U S A, 1996. 93(21): p. 11295-301.
66. Querido, E., et al., *Degradation of p53 by adenovirus E4orf6 and E1B55K proteins occurs via a novel mechanism involving a Cullin-containing complex.* Genes Dev, 2001. 15(23): p. 3104-17.
67. Stracker, T.H., C.T. Carson, and M.D. Weitzman, *Adenovirus oncoproteins inactivate the Mre11-Rad50-NBS1 DNA repair complex.* Nature, 2002. 418(6895): p. 348-52.
68. Ciechanover, A., *The ubiquitin-proteasome pathway: on protein death and cell life.* EMBO J, 1998. 17(24): p. 7151-60.
69. Pickart, C.M., *Targeting of substrates to the 26S proteasome.* FASEB J, 1997. 11(13): p. 1055-66.
70. Conze, D.B., et al., *Lys63-linked polyubiquitination of IRAK-1 is required for interleukin-1 receptor- and toll-like receptor-mediated NF-kappaB activation.* Mol Cell Biol, 2008. 28(10): p. 3538-47.
71. Lim, K.L., et al., *Parkin mediates nonclassical, proteasomal-independent ubiquitination of synphilin-1: implications for Lewy body formation.* J Neurosci, 2005. 25(8): p. 2002-9.
72. Lim, K.L., V.L. Dawson, and T.M. Dawson, *Parkin-mediated lysine 63-linked polyubiquitination: a link to protein inclusions formation in Parkinson's and other conformational diseases?* Neurobiol Aging, 2006. 27(4): p. 524-9.
73. Olzmann, J.A., et al., *Parkin-mediated K63-linked polyubiquitination targets misfolded DJ-1 to aggresomes via binding to HDAC6.* J Cell Biol, 2007. 178(6): p. 1025-38.
74. Sheaff, R.J., et al., *Proteasomal turnover of p21Cip1 does not require p21Cip1 ubiquitination.* Mol Cell, 2000. 5(2): p. 403-10.
75. Chew, E.H. and T. Hagen, *Substrate-mediated regulation of cullin neddylation.* J Biol Chem, 2007. 282(23): p. 17032-40.
76. Allander, T., *Human bocavirus.* J Clin Virol, 2008. 41(1): p. 29-33.
77. Chen, A.Y., et al., *Characterization of the gene expression profile of human bocavirus.* Virology. 403(2): p. 145-54.

78. Carmichael, L.E., D.H. Schlafer, and A. Hashimoto, *Pathogenicity of minute virus of canines (MVC) for the canine fetus.* Cornell Vet, 1991. 81(2): p. 151-71.
79. Binn, L.N., et al., *Recovery and characterization of a minute virus of canines.* Infect Immun, 1970. 1(5): p. 503-8.
80. Qiu, J., et al., *The transcription profile of the bocavirus bovine parvovirus is unlike those of previously characterized parvoviruses.* J Virol, 2007. 81(21): p. 12080-5.
81. Lederman, M., et al., *Virally coded noncapsid protein associated with bovine parvovirus infection.* J Virol, 1984. 49(2): p. 315-8.
82. Lederman, M., R.C. Bates, and E.R. Stout, *In vitro and in vivo studies of bovine parvovirus proteins.* J Virol, 1983. 48(1): p. 10-7.
83. Choi, E.Y., et al., *Replication of minute virus of mice DNA is critically dependent on accumulated levels of NS2.* J Virol, 2005. 79(19): p. 12375-81.
84. Venkatesh, L.K., O. Fasina, and D.J. Pintel, *RNAse mapping and quantitation of RNA isoforms.* Methods Mol Biol. 883: p. 121-9.
85. Guan, W., et al., *Block to the production of full-length B19 virus transcripts by internal polyadenylation is overcome by replication of the viral genome.* J Virol, 2008. 82(20): p. 9951-63.
86. Walker, S.L., R.S. Wonderling, and R.A. Owens, *Mutational analysis of the adeno-associated virus type 2 Rep68 protein helicase motifs.* J Virol, 1997. 71(9): p. 6996-7004.
87. *PARVOVIRUSES*. 6th edition ed. The evolution of Parvovirus taxonomy, ed. P. Tattersall. 2006, United Kingdom: Hodder Arnold.
88. Shepard, P.J. and K.J. Hertel, *The SR protein family.* Genome Biol, 2009. 10(10): p. 242.
89. Pintel, D., et al., *The genome of minute virus of mice, an autonomous parvovirus, encodes two overlapping transcription units.* Nucleic Acids Res, 1983. 11(4): p. 1019-38.
90. Mouw, M.B. and D.J. Pintel, *Adeno-associated virus RNAs appear in a temporal order and their splicing is stimulated during coinfection with adenovirus.* J Virol, 2000. 74(21): p. 9878-88.
91. Liu, Z., et al., *Comparison of the transcription profile of simian parvovirus with that of the human erythrovirus B19 reveals a number of unique features.* J Virol, 2004. 78(23): p. 12929-39.
92. Guan, W., et al., *Internal polyadenylation of the parvovirus B19 precursor mRNA is regulated by alternative splicing.* J Biol Chem, 2011. 286(28): p. 24793-805.
93. Qiu, J., et al., *The transcription profile of Aleutian mink disease virus in CRFK cells is generated by alternative processing of pre-mRNAs produced from a single promoter.* J Virol, 2006. 80(2): p. 654-62.
94. Huang, Q., et al., *Internal polyadenylation of parvoviral precursor mRNA limits progeny virus production.* Virology. 426(2): p. 167-77.

# VITA

Loretta Sukhu was born in the county of Berbice, British Guyana, the youngest of eight children. Loretta completed a Bachelor's of Science degree in Biochemistry at the University of Manitoba in Winnipeg, Canada. Following graduation Loretta took a position at the Hospital for Sick Children in Toronto and continued her research at the University of Florida on the role of microfilaments in the metastasis of glioblastoma tumors and help establish the Southeastern Brain Tumor Tissue Repository. In 1993 Loretta took a position with Vical Inc., a small biotechnology company in San Diego where she stayed for the next eleven years. During her time at Vical she implemented and managed a fully equipped GMP compliant cell culture facility, developed cell-based and immunoassays for product development, co-authored US patent # 6,875,748 as well as multiple peer-reviewed publications in the fields of DNA vaccine and in vivo plasmid DNA delivery research. In 2006 Loretta began her graduate work in the laboratory of Dr. David Pintel in the Department of Molecular Microbiology and Immunology at the University of Missouri in Columbia, Missouri.

Loretta currently lives in Columbia Missouri with her husband of 16 years Dan Hassett, their son Luke, two cats, and many tropical fish.